

**DEVELOPMENT OF HYBRID ALUMINIUM AIR BATTERY-FUEL
CELL SYSTEM**

KHOR ZHENG YU

**A project report submitted in partial fulfilment of the
requirements for the award of Bachelor of Engineering
(Honours) Mechanical Engineering**

**Lee Kong Chian Faculty of Engineering and Science
Universiti Tunku Abdul Rahman**

May 2020

DECLARATION

I hereby declare that this project report is based on my original work except for citations and quotations which have been duly acknowledged. I also declare that it has not been previously and concurrently submitted for any other degree or award at UTAR or other institutions.

Signature : 证滢

Name : Khor Zheng Yu

ID No. : 15UEB05467

Date : 15/5/2020

APPROVAL FOR SUBMISSION

I certify that this project report entitled “**DEVELOPMENT OF HYBRID ALUMINIUM AIR BATTERY-FUEL CELL SYSTEM**” was prepared by **KHOR ZHENG YU** has met the required standard for submission in partial fulfilment of the requirements for the award of Bachelor of Engineering (Honours) Mechanical Engineering at Universiti Tunku Abdul Rahman.

Approved by,

| | | |
|------------|---|--------------------------|
| Signature | : | <i>Bernard Saw</i> |
| | | _____ |
| Supervisor | : | Dr. Bernard Saw Lip Huat |
| | | _____ |
| Date | : | 15/5/2020 |
| | | _____ |

The copyright of this report belongs to the author under the terms of the copyright Act 1987 as qualified by Intellectual Property Policy of Universiti Tunku Abdul Rahman. Due acknowledgement shall always be made of the use of any material contained in, or derived from, this report.

© 2020, Khor Zheng Yu. All right reserved.

ACKNOWLEDGEMENTS

I would like to thank everyone who had contributed to the successful completion of this project. I would like to express my gratitude to my research supervisor, Dr. Bernard Saw Lip Huat for his invaluable advice, guidance and his enormous patience throughout the development of the research. Also, thanks to my friends for lending me their selfless knowledge and providing me guidance to achieve the aim and objectives of this study.

In addition, I would also like to express my gratitude to my loving parents and friends who had helped and given me encouragement during the period of my research.

ABSTRACT

Due to the constant increase in electric demand of our society, new energy production, transport and storage systems will play a key role in a near future. Regarding to energy storage systems, electrochemical energy storage is a potential candidate because of direct conversion from chemical energy to electrical energy and vice versa. Aluminium is a very promising energy carrier given its high capacity and energy density, low cost, earth abundance and environmental benignity. Traditional aluminium air battery experiences impediment from the self-corrosion and related safety problems. In this study, a new approach was proposed to ameliorate the issue and developed to study the performance of the cell; by incorporating an additional hydrogen-air fuel cell into the system. The hybrid system turned the self-corrosion issue into a beneficial reaction by utilizing the hydrogen gas produced from aluminium for fuel cell. 2-electrode and 3-electrode configuration were employed using LSV technique to obtain cell polarization curve. The hybrid cell displayed significant improvement after integrating the fuel cell, the open circuit voltage was 1.3 V and power output increases by 44 % from 6.20 mW – 8.93 mW. From the polarization curve, the cell was limited by overpotential loss such as ohmic loss, activation loss and mass transport loss. Optimization was carried out to augment the performance of the hybrid cell. The hydrogen anode and cathode air were changed to graphite felt, besides, increasing the dimension of air cathode to increase intake of ambient air. The optimized cell recorded an additional increase of 10.67 mW compare to carbon cloth-based cathode. Aluminium utilization test was conducted with different concentration of electrolyte and utilization efficiency is able to reach up to 90.2 %. The maximum power density of the entire hybrid system increases significantly by over 20% after incorporating the hydrogen-air sub cell; the increase was even significant with higher concentration of electrolyte. The hybrid system is adaptable in concentrated alkaline electrolyte with significantly improved power output at no sacrifice of its overall efficiency. Discharge cell efficiency was tested at 10 mA, 20 mA and 50 mA the discharge efficiency of the hybrid cell range from 75.4 % - 91.7 %.

TABLE OF CONTENTS

| | | |
|--|--|-------------|
| DECLARATION | | i |
| APPROVAL FOR SUBMISSION | | ii |
| ACKNOWLEDGEMENTS | | iv |
| ABSTRACT | | v |
| TABLE OF CONTENTS | | vi |
| LIST OF TABLES | | viii |
| LIST OF FIGURES | | ix |
| LIST OF SYMBOLS / ABBREVIATIONS | | xi |
| LIST OF APPENDICES | | xii |
| | | |
| CHAPTER | | |
| 1 | INTRODUCTION | 1 |
| 1.1 | General Introduction | 1 |
| 1.2 | Importance of the Study | 3 |
| 1.3 | Problem Statement | 4 |
| 1.4 | Aim and Objectives | 5 |
| 1.5 | Scope and Limitation of the Study | 5 |
| 1.6 | Contribution of the Study | 6 |
| 1.7 | Outline of the Report | 6 |
| 2 | LITERATURE REVIEW | 7 |
| 2.1 | Introduction | 7 |
| 2.2 | Fuel cell technologies development | 8 |
| 2.3 | The Development of Metal-air Batteries | 12 |
| 2.4 | Development of Aluminium-air battery | 16 |
| 2.5 | Aluminium Alloys | 19 |
| 2.6 | Cathode Electrode | 20 |
| 2.7 | Electrolytes of Aluminium-air battery | 21 |
| 2.7.1 | Alkaline Electrolyte | 22 |

| | | | |
|----------|-------|--|-----------|
| | 2.7.2 | Correlation of electrolyte concentration and battery performance | 23 |
| | 2.7.3 | Inhibitor and Other Types of Electrolyte | 23 |
| | 2.8 | Aluminium as source of hydrogen for fuel cell | 24 |
| 3 | | METHODOLOGY AND WORK PLAN | 27 |
| | 3.1 | Introduction | 27 |
| | 3.2 | Design of Prototype | 28 |
| | 3.3 | Materials Preparation | 29 |
| | 3.4 | System Fabrication | 30 |
| | 3.5 | Preliminary Test | 31 |
| | 3.6 | Optimization Test | 33 |
| | 3.7 | Verification of Hydrogen Gas Test | 33 |
| | 3.8 | Aluminium Utilization Test | 34 |
| | 3.9 | Performance on Optimised Cell Test | 35 |
| 4 | | RESULTS AND DISCUSSION | 36 |
| | 4.1 | Introduction | 36 |
| | 4.2 | Preliminary Test | 37 |
| | 4.2.1 | Performance of Aluminium/air Sub-cell | 37 |
| | 4.2.2 | Hydrogen/air Sub-cell Performance | 38 |
| | 4.3 | Hydrogen gas test | 42 |
| | 4.4 | Optimization | 43 |
| | 4.4.1 | Optimization on the type of electrodes | 43 |
| | 4.5 | Aluminium Utilization Test | 46 |
| | 4.6 | Performance on Optimize System | 53 |
| | 4.6.1 | Performance of Aluminium-air Sub-cell | 53 |
| | 4.6.2 | Performance of Hydrogen/air Sub-cell | 54 |
| | 4.6.3 | Overall System Efficiency Performance | 55 |
| | 4.6.4 | Discharge Test Evaluation | 58 |
| 5 | | CONCLUSIONS AND RECOMMENDATIONS | 61 |
| | 5.1 | Conclusions | 61 |
| | 5.2 | Recommendations for future work | 62 |
| | | REFERENCES | 64 |
| | | APPENDICES | 70 |

LIST OF TABLES

| | |
|---|----|
| Table 4.1: Data for Volume of Hydrogen Gas Collected, Mass of Aluminium Used, Hydrogen Generation Rate, and Efficiency at 1M Concentration. | 47 |
| Table 4.2: Peak Power Densities of Hybrid System. | 56 |
| Table 4.3: Efficiency of Hybrid System at Peak Power Densities. | 57 |
| Table 4.4: The Discharge Efficiency of Cell at Different Discharge Current. | 59 |

LIST OF FIGURES

| | |
|---|----|
| Figure 2.1: A schematic diagram of a battery and fuel-cell (Winter and Brodd, 2004). | 8 |
| Figure 2.2: The power density and energy density for different energy storage (Winter and Brodd, 2004). | 10 |
| Figure 2.3: The schematic diagram of a typical metal-air battery (Zhang et al., 2016). | 13 |
| Figure 2.4: Historical development of aluminium-air battery (Liu et al., 2017). | 17 |
| Figure 2.5: The current density, cell voltage and power density with different concentration of electrolyte (Wang et al., 2013). | 23 |
| Figure 2.6 : Working principle of the hybrid system from energy view point (Yang and Knickle, 2002). | 26 |
| Figure 3.1: Work Flowchart | 28 |
| Figure 3.2: Prototype Design (left) Cross-section Area of Hybrid Cell (right) | 29 |
| Figure 3.3: Laser cutter machine for slicing Perplex glass. | 30 |
| Figure 3.4: Hydrogen collector (left) Prototype of aluminium-air battery fuel-cell (right). | 31 |
| Figure 3.5: Experiment Setup for Performance Test. Connection from Work Station to the Al/air Sub-cell. | 32 |
| Figure 3.6: Carbon Cloth Single Electrode Polarization Test Setup. Reference Electrode (RE), Counter-Electrode (CE) and Working Electrode (WE) was connected to Ag/AgCl, Aluminium and Carbon Cloth respectively. | 33 |
| Figure 3.7: Efficiency Testing Setup. The test rig was connected to the hydrogen collector by the plastic tube. | 35 |
| Figure 4.1: Electrochemical reaction of aluminium in alkaline solution. | 37 |
| Figure 4.2: Polarization Curve of Aluminium/air Sub-cell. | 37 |
| Figure 4.3: Single electrode polarization data of Aluminium/air Sub-cell. | 39 |
| Figure 4.4: Polarization Curve of Hydrogen/air Sub-cell. | 40 |

| | |
|--|----|
| Figure 4.5: Single Electrode Polarization Data of Hydrogen anode/air Sub-cell measure vs Ag/AgCl as Reference Electrode. | 40 |
| Figure 4.6: The Polarization Curve Classified into Respective Loss. | 42 |
| Figure 4.7: Polarization Curve between Carbon cloth(previous) and Graphite(new) at Aluminium/air Sub-cell. | 44 |
| Figure 4.8: Standard Electrode Polarization Data between Carbon Cloth (dashed line) and Graphite Felt at Aluminium/air Sub-cell. | 44 |
| Figure 4.9: Polarization Curve between Carbon cloth(previous) and Graphite(new) at Hydrogen/air Sub-cell. | 45 |
| Figure 4.10: Standard Electrode Polarization Data between Carbon Cloth (dashed line) and Graphite Felt at Hydrogen/air Sub-cell. | 46 |
| Figure 4.11: Hydrogen Generation Rate vs Voltage in Different Concentration of KOH. | 49 |
| Figure 4.12: Aluminium Utilization Efficiency vs Voltage in Different Concentration of KOH. | 49 |
| Figure 4.13: Theoretical model of aluminium reaction in alkaline solution. | 51 |
| Figure 4.14: Images of Aluminium foil using SEM. (a) Aluminium kitchen foil before reaction (b) Aluminium foil after 24 hours of experiment. | 52 |
| Figure 4.15: EDX analysis and atomic weight composition on Aluminium (a) Before reaction (b) After 24hours of experiment. | 52 |
| Figure 4.16: Polarization Curve of Aluminium/air Sub cell with Different Electrolyte Concentration. | 54 |
| Figure 4.17: The Polarization curve of Hydrogen/air Sub-cell with Different Electrolyte Concentration | 55 |
| Figure 4.18: The Maximum Power Achieved at Different Concentration of Electrolyte. | 56 |
| Figure 4.19: Graph of Voltage Output against Current Capacity at 10 mA, 20 mA and 50 mA Discharge Rate. | 59 |

LIST OF SYMBOLS / ABBREVIATIONS

| | |
|------------------|--|
| r_H | hydrogen evolution rate, $\mu\text{L/s}$ |
| ε | efficiency |
| P_{max} | Maximum Power, mW |
| \bar{e} | electron |
| ESS | Energy Storage System |
| PEMFC | Proton-exchange Membrane Fuel Cell |
| MCFC | Molten Carbonate Fuel Cell |
| SOFC | Solid Oxide Fuel Cell |
| AFC | Alkaline Fuel Cell |
| Al | Aluminium |
| Ga | Gallium |
| In | Indium |
| Sn | Tin |
| Zn | Zinc |
| GDE | Gas Diffusion Electrode |
| OCV | Open Circuit Voltage |
| LiB | Lithium-ion battery |
| H ₂ O | Water Molecules |
| H ₂ | Hydrogen gas |
| O ₂ | Oxygen molecules |
| KOH | Potassium Hydroxide |
| OH ⁻ | Hydroxide ion |
| M | Molarity |
| Ag/AgCl | Silver/ Silver Chloride |
| LSV | Linear Sweep Voltammetry |

LIST OF APPENDICES

| | |
|--|----|
| APPENDIX A: The conceptual design of hybrid system | 70 |
| APPENDIX B: Specific conductivity of KOH at different temperature and concentration. | 70 |

CHAPTER 1

INTRODUCTION

1.1 General Introduction

The dominant primary energy source, fossil fuel, supplying 85% of mankind's energy demand ranging from industrial to transportation has leads to rapid depletion of resources (Dehghani-Sanij, 2017). Internal combustion engine operates at high level power density, outperforming vehicles that utilize electrochemical energy system. Growing human demand activities consequently, leads to damage on the environment such as global warming, climate change, air pollution, major health impacts and other risk of environment contaminations. The burning of fossil fuel causes the emission of carbon dioxide (CO₂) to rose from 6.4 Gt C in 1995 (gigatons of carbon) to 9.8 Gt C in 2013 (Bonde, 2016).

The dwindling of global fossil fuel supply and surge of atmospheric carbon concentration has driven various advancements of electrochemical energy system in automobile industry. Currently, hybridization of energy storage system (ESS) is one of the ongoing research lines that attract more attention from researches (Gauchia et al., 2011). ESS comprises of batteries, electrochemical capacitors, also known as supercapacitor, and fuel cells (Winter and Brodd, 2004a).

The three energy storages undergo almost similar electrochemical process that involves the diffusion and transfer of ions between two different electrodes at the phase boundary of the electrolyte. Batteries and fuel cells will undergo chemical reaction in an electrolyte via redox reaction to generate electrical energy. The difference between them is related to the type of system and the role of electrode. Battery is a closed system whereby the electrodes will be stored in the same compartment and undergo redox reaction. On the other hand, fuel cell is an open system where the electrodes are just media for charge transfer and redox reaction occurs externally. Supercapacitor uses large carbon-based electrode to accumulate ions via electrostatic interaction forming electrical double layers (EDLs) at the electrolyte interface (Li et al., 2014).

Energy delivery process will occur in the external wire due to the movement from the electrons.

Contrary to supercapacitors and fuel cells, batteries have been well developed and being implemented widely in myriad application. Supercapacitors have found niche markets in electronic devices such as volatile memory backups in computer and uninterruptible power supplies (Libich et al., 2018). Fuel cells have been incorporated into automobile replacing battery, which are known as Fuel Cell Electric Vehicle (FCEV). Batteries is being widely utilize in various application especially automobiles due to their characteristics, ranging from reliability and performance to compact design (Khaligh and Li, 2010).

Researchers have developed many kinds of battery to suit different application. Lead-acid battery has been widely implemented in hybrid electric vehicle (HEV) due to its unique characteristics such as maintenance free, ability to withstand overcharging and offer the longest life cycle. However, the energy density of the battery is still relatively low and the battery faces dwindle life cycle in deep rate of discharge. In nickel-metal hydride (NiMH) battery, the energy density is two times bigger than lead acid battery. The traits of NiMH are environmentally friendly, recyclable and possess higher volumetric energy and power than lead acid battery. However, if the load current is being discharged repeatedly, the life will be reduced by 200 - 300 cycles (Wehrey, 2004). In lithium-ion battery, some of the promising aspects that it provides is a low memory effect, high specific power and long battery life. Although it is proven to have excellent performance, the price of owning one is relatively high.

For the past few years, metal air battery has become the focus of research mainly due to its high efficiency and clean energy. There are several mainstream metal-air that are undergoing research, such as zinc-air battery, aluminium-air battery, magnesium-battery and lithium-air battery.

In this research endeavour, aluminium-air battery is being investigated. Aluminium-air battery is an electrochemical energy storage system that produce electricity from chemical energy. The aluminium anode reacts with electrolyte while the air cathode will be exposed to ambient air in order to react with oxygen. The anode experiences corrosion due to parasitic reaction on the surface of aluminium, leading to the production of hydrogen gas. This hydrogen gas can

be used as fuel for fuel cell. In this system, Alkaline Fuel Cell (AFC) will be incorporated with the Al-air battery. Comparing among the metal-air batteries, Al-air is regarded as one of the highest energy densities (Briguglio et al., 2011). Its' application was limited for military application due to its by-product from anodic reaction. As time pass, more suitable electrolyte has been developed and more solutions have been proposed to solve the problem. It has advantages of high theoretical voltage (2.7 V), high energy density (8100 Wh kg⁻¹) and capacity (2980 mA h g⁻¹) (Liu et al., 2017a). One of the current fields that started utilizing Al-air battery is the automobile industry. An electric vehicle was tested with aluminium batteries and was proven to be capable of travelling up to eight times the distance travelled by a lithium-ion battery (Yang, 2003).

1.2 Importance of the Study

In the early 1990s, Lithium-ion batteries (LiB) were commercialized to replace nickel-cadmium batteries that were found in portable equipment for electronic components. LiB have been developed progressively over the past few years. Due to the battery's attribute, it was implemented for vast application ranging from electronic devices to vehicles. The US Department of Energy has demanded that battery should have energy density of more than 400 Wh/kg, unfortunately, the state-of-the-art commercial LiB are only 227 Wh/kg (Chawla, 2017). Apart from the aforementioned setback faced by the LiB, it encounters another two limitations:

- Safety concern. Although LiB can store a lot of energy than other rechargeable batteries, it is a highly reactive and flammable element. This may lead to explosion if not handle carefully. An aqueous-based electrolyte required protection circuitry to be added to ensure they function within a safe operating limit (Padbury and Zhang, 2011).
- Cost. One of the major disadvantages is their affordability. The cost to manufacture one lithium ion is four to eight times costlier than a lead acid battery and one to four times for nickel-metal hydride cell. The cost will be significant as it will be mass produced, thus, any additional cost should be considered.

Following the increase of human activities demand and technology evolution, a more sophisticated battery that can satisfy the needs of systems are required. Extensive amount of time has been poured in developing battery technology in order to meet the increasing requirements of battery storage. Researchers is endeavouring in coming up with a battery that offer high energy density, long cycle life, affordable and environmentally benign. Aluminium-air batteries seems to be the favourable candidate that can fulfil all the criteria. However, they are not widely implemented due to the self-corrosion reaction on the anode and non-rechargeable issue.

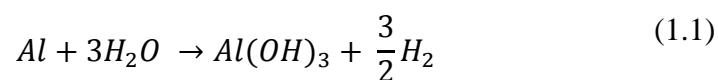
The results of this present study may have significant impact on providing alternative way to improve the performance of aluminium-air battery. It aims to investigate how adding fuel cell into Al-air-battery affects the efficiency of the whole system. In addition, this research can lead to a better understanding on the theory behind:

- The electrochemical reaction at anode and cathode electrode in the aluminium-air battery fuel cell system.
- The working principle of an aluminium-air battery-fuel cell system.

1.3 Problem Statement

Aluminium-air battery-fuel cell is a promising renewable energy storage system. Several serious problems exist that limits the usage of Al-air cells to be implemented in vast application is explained below:

Parasitic reaction from anode. During discharge, the main reaction is between aluminium anode and air cathode. However, a sub reaction occurs simultaneously; the parasitic hydrogen evolution as shown in Eq. 1.1. Consequently, the performance of cell decreases due to retardation of mass transfer at the cathode and reduction in conductivity.



The concentration of alkaline electrolyte will affect the corrosion rate of aluminium. When using a higher concentration electrolyte, more hydrogen is being produced that can be utilized by the fuel cell. However, a higher corrosion means the aluminium will corrode faster hence it is best to choose an optimal solution.

Fuel cell is an electrochemical cell that converts chemical energy of a fuel (hydrogen gas) and an oxidizing agent (oxygen) into electricity via redox reaction. In this project, fuel cell will be incorporated into the system and turning the unfavourable parasitic reaction into beneficial product by utilizing the hydrogen gas produced for fuel cell.

1.4 Aim and Objectives

The main aim of this research is to study the improvisation on the conventional aluminium-air battery by adding an additional feature which comprises the fuel cell. This research target to increase the performance of battery by utilizing the hydrogen gas from anodic corrosion for fuel cell. This battery-fuel cell will be more efficient as it produces better metal utilization. In order to fulfil the main aim for this paper, specific objectives needed to be achieved:

1. To design and construct the hybrid aluminium-air battery-fuel cell system. Design a prototype that fit both aluminium-air sub cell and hydrogen-air sub cell (fuel cell) in a single test rig. A hydrogen compartment is needed to store the excessive hydrogen gas produced from aluminium anode.
2. To analyse the electric performance of the aluminium-air battery-fuel cell system.
3. To analyse the performance of the aluminium-air battery-fuel cell system. Analyse the overall efficiency of the hybrid cell from its' polarization curve.

1.5 Scope and Limitation of the Study

In order to achieve the aim and objectives, scopes needed to be determined to reach the goal. The scopes of this study will be focusing on designing, fabricating, modifying the aluminium air battery fuel cell prototype. The

hydrogen produced from the aluminium anode will be utilized for fuel cell to increase the efficiency of the overall system. The composition of the gas produced from the anode is tested.

Cost is the biggest limitation in this study because it has put a constrain on the selection of material for cathode as the material used must have platinum catalyst in order for the gas molecules to diffuse through the porous layer and undergo redox reaction. Besides, it is hard to search for supplier in Malaysia, this leave only an option which is to import the material from overseas.

Moreover, the compartment that trap hydrogen gas may not captured all of the gas that is released by the aluminium anode. Some of the gas may leave through the inlet for electrolyte, consequently, the efficiency result may be affected.

1.6 Contribution of the Study

The contribution of this project may help to mitigate the problem from the parasitic reaction occurs by the aluminium-air battery when reacts with alkaline medium. A hydrogen/air sub-cell, acting as the fuel cell, is embedded into the tandem cell system to utilize the hydrogen gas produced from the aluminium-air battery.

1.7 Outline of the Report

In this report, literature review has been discussed and commented in Chapter 2. Methodology, experimental set up, and prototypes' designs have been explained in Chapter 3. Furthermore, results obtained from the performance of aluminium-air battery fuel cell has been recorded and discussed in Chapter 4. The conclusions and recommendations have been presented in Chapter 5.

CHAPTER 2

LITERATURE REVIEW

2.1 Introduction

Energy storage system is undergoing evolution at a rapid pace. Due to environmental pollution and increasing human activity demand, more advance and environmentally friendly battery is required to overcome these issues. Conventional battery technologies show little promise to fulfil the desire outcome for application that required higher power and energy density at affordable cost.

Currently, modern society is having paradigm shift in energy storage industry from depleting fossil fuel to a more sustainable energy alternatives in order to combat global warming and environmental pollution (Pollet, Staffell and Shang, 2012). Eco-friendly batteries are the most sought out solution to be commercialize in large scale production. The fuel and oxidant substance generate electrical energy at high efficiency by undergoing chemical reaction at the expense of limited energy density. In a combustion engine, to produce electrical energy, the fuel and the oxidant is first being converted into mechanical energy in the form of heat from chemical energy. The mechanical energy can be directly used to power a car or further convert into electrical energy by generator (Strauß, Vetter and Von Felde, 2012). In comparison with the battery, the efficiency of combustion engine is lower but it was compensated by the high energy density. Fuel cell, stands at the intersection of both battery and combustion engine, produces electrical energy directly from chemical energy where oxidant is stored at another chamber. Unfortunately, it faces many problems that hinders the development of fuel cell.

Therefore, developing better electrochemical energy technologies is important and crucial. Metal-air battery has attracted much attention due to its large capacity, eco-friendly, long life cycle and rechargeable characteristics. Metal-air battery, an electrochemical cell, utilize certain metal element as anode and take in ubiquitous oxygen from the air to generate electricity. The anode works the same as a battery negative electrode while the cathode will undergo reaction which is similar to an air-based fuel cell. The use of catalyst is optional

for the anode reaction, which could improve the performance of cell at the expense of cost. Meanwhile, a high energy density air-battery could be achieved using certain metal anodes depending on its chemical properties. Among various anode candidates for metal-air batteries, tremendous research efforts have been done on lithium-air battery as it has highest theoretical energy densities among the air batteries (Goodenough, 2014). However, due to its safety concern and scarcity of element available, aluminium is thought to be very promising as it possesses high energy density, superior safety, environment benignity, recyclable, and possess abundance in the Earth's crust.

2.2 Fuel cell technologies development

In the mid-18th century, fuel cell has been established despite their modern technology aura. The first commercialize fuel cell was one century later when NASA used it in spacecraft for power generation and drinking water. It was being commercialized in electric vehicle in 2007(Lucia, 2014). Fuel cell have evolved dramatically for past few years, various types of fuel cell made from different electrolyte have been invented for different purpose. Even so, the fundamental working principle of the fuel cell remains the same. As display in Figure 2.1, the schematic diagram shows the comparison between a battery and fuel cell (Winter and Brodd, 2004). Although their working mechanism are different, but they shared the similar fundamental electrochemical principles.

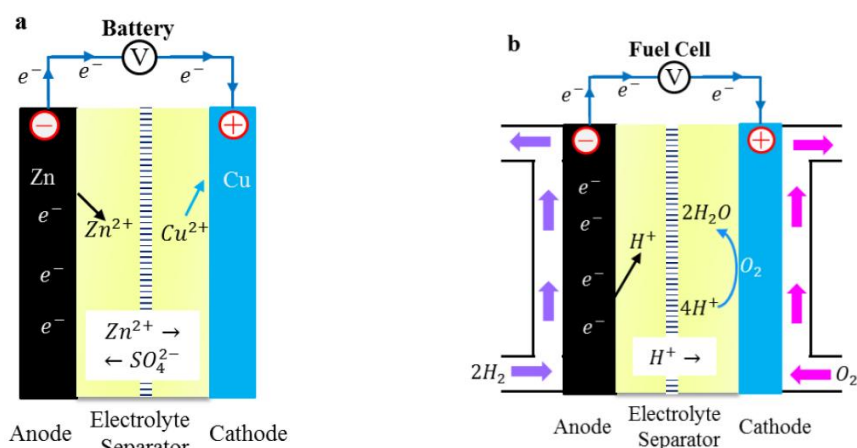


Figure 2.1: A schematic diagram of a battery and fuel cell (Winter and Brodd, 2004).

A fuel cell undergoes electrochemical reactions to generate electricity by converting the chemical energy residing in a fuel. A fuel cell shares the traits of both combustion engine and battery while combining the advantages of both. When producing electricity, the refillable fuel (hydrogen gas and oxygen) will undergo redox at anode and cathode similar to a battery and combustion engine. Fuel cell differ from batteries in which the continuous supply of fuel comes from an external source and not within the fuel cell compartment (the place where redox reaction occurs) (Brett et al., 2006). Therefore, fuel cell is classified as open system while battery is considered as closed system. The fuel commonly used by fuel cell is hydrogen gas. Although both fuel cell and combustion engine are open system, but their power generation mechanism differ from one another with unique individual characteristic. In a combustion engine, heat from combustion (chemical energy) is converted to push the piston shaft (mechanical energy) that is connected to the generator (electrical energy). On the other hand, fuel cell is able to convert from hydrogen (chemical energy) directly to electricity. Researchers noticed that a regular internal combustion engine has an overall conversion efficiency of 20 %. In contrast to a fuel cell which is able to utilize its fuel more efficiently, around 40 % (Cells et al., 2013).

Figure 2.2 shows the graph of power density against energy density for different energy storage systems (Winter and Brodd, 2004). Fuel cells depicts lowest specific power but was offset by having competitively large specific energy density. Therefore, with such huge storage capacity fuel cell is suitable to be an electrical storage for intermittent renewable resources like solar and hydroelectric. A fuel cell is able to store and produce electrical energy just like a battery, the difference between them is, the former is an open system while the latter is a close system. A close system has limited amount of fuel to undergo electrochemical reaction while an open system will have continuous supply of fuel providing to the system (Schmidt-Rohr, 2018).

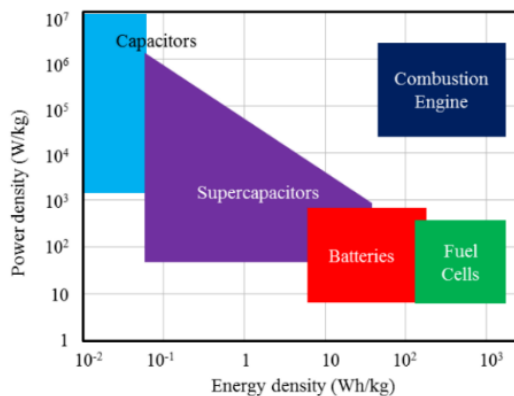


Figure 2.2: The power density and energy density for different energy storage (Winter and Brodd, 2004).

A fuel cell is composed of three segments: an anode, a cathode and an electrolyte that is sandwiched between them. Hydrogen fuel will be supplied to the anode and oxidized by a catalyst. The atom will break into positively charge ion and negatively charge electron. The ions will move to cathode via electrolyte and undergo chemical reaction producing water or carbon dioxide. Electron is produced and travel to the cathode via the external wire, creating an electrical current. A single unit cell only has potential of 0.5 V to 0.8 V which is insufficient for most application. However, if stacked up, they are able to increase the voltage by severalfold depending on the number of stack-up cells (Kane, Mishra and Dutta, 2016).

Fuel cell is being categorize in relation to their electrolyte materials. Some of the well-known fuel cells are PEMFC, MCFC (molten carbonate fuel cell), SOFC (solid oxide fuel cell) and AFC (alkaline fuel cell). According to reports on the application of fuel cell (Lucia, 2014), the availability of fuel cell in the market has rose by 40 %, 95 % of which is portable fuel cell and PEMFC accounted to 97 % of fuel cell technology. SOFC usually operates at high temperature and run on variety of fuel such as hydrogen, ammonia and natural gas. The ability to withstand high temperature is due to its ceramic electrolyte making it is suitable for auxiliary power units in vehicles, power generation for power plants and commercial energy system.

Although PEMFC and SOFC are more widely known compare to other fuel cells. PEMFC consider to be a suitable substitute for battery due to its high efficiency, high power density and sustainable materials. Unfortunately, with

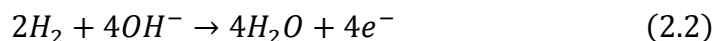
the state-of-art of fuel cell, battery technology still has the upper hand for massive applications because the fuel cell raises issues on affordability, technology uncertainty and safety concern. By comparing electrical vehicle in 2010, the electrical storage system in a Battery Electric Vehicle (BEV) would cost USD 26,700 while a Fuel Cell Electric Vehicle (FCEV) could cost up to USD 47,400 (Offer et al., 2010). Besides, safety concern of using hydrogen as fuel for fuel cell is another reason for public to turn away from using fuel cell technology. As such, more and more researches are being conducted to improve the stability and performance of fuel cell. Several other issues have been addressed to the Research and Development focusing on various academic aspect such as (Sharaf and Orhan, 2014):

- Enhance or develop electrolyte materials that have better conductivity and stability under different circumstances (high temperature and high humidity).
- Design high tolerance impurities membrane.
- Inventing a much more durable seal for high-temperature fuel cell.
- Develop catalyst that can be utilized for all types of fuel cell.
- Eliminate corrosion on bipolar plates with coatings.
- Enhance model stack durability and reduce degradation.

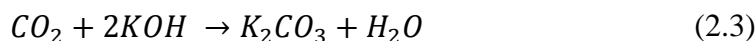
Alkaline fuel cell was developed back in the 1960, it was use in the space shuttle from NASA to supply electric power on-board. Pure hydrogen and common alkaline solution for electrolytes used in AFC are sodium hydroxide (NaOH) and potassium hydroxide (KOH). One of the forte of using AFC is that the alkaline electrolyte is much more favourable for oxygen reduction which in turn produce higher voltage in the unit. Both anode and cathode differ significantly from PEMFC attributed from the electrochemical half-cell reactions. Hydroxide anions (OH^-) are formed at the cathode by receiving oxygen and water as shown in equation 2.1.



The anode will then undergo oxidation when OH^- flow from cathode to the anode, reacting hydroxide ion with hydrogen gas. Water and electrons are produced as shown in equation 2.2.



One major downside of AFC is poisoning of electrolyte by carbon dioxide (CO_2). When CO_2 reacts with the electrolyte, carbonates are formed as shown in Eq.2.3. This reaction reduces the number of available OH^- for reaction and reduces the ionic conductivity of the electrolyte solution. The carbonates would block the porous electrode decreases the performance of the fuel cell. One of the solutions was to incorporate a “scrubber” which will filter the air and only allows oxygen to enter the electrode or install pump for circulation the electrolyte (Fain, 2015).



2.3 The Development of Metal-air Batteries

A metal air battery is another variant of battery that uses electrode comprises of metal element to generate electricity. It is consider as a unique type of fuel cell that utilizes metal as anode and air as fuel for reduction (Chen et al., 2009). The cell comprises of an air cathode, metal anode, separator and an electrolyte. The electrodes will undergo redox reaction converting the chemical reaction into electrical generating system.

As depicts in Figure 2.3, when the external circuit of the battery is connected, oxidation and reduction take place between the anode and cathode respectively (Zhang et al., 2016). During the discharge cycle, anode will undergo oxidation in which pure metal will be oxidized and produce proton and electron. The proton will flow to the cathode through electrolyte while the electron is being transported via the external circuit. The gas diffusion cathode is a carbon based structure that takes in oxygen from ambient air and reacts with water, resulting in reduction of the oxygen (Ding et al., 2016). Metal-air batteries have been be implemented in myriad application, some of the merits include exceptional high energy density, rechargeable system and lower cost.

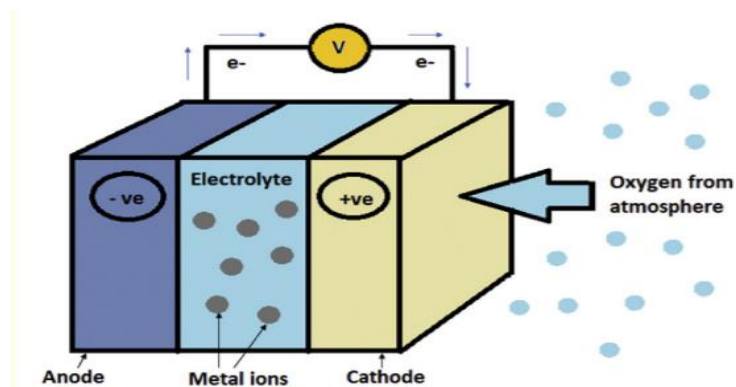


Figure 2.3: The schematic diagram of a typical metal-air battery (Zhang et al., 2016).

Currently, the development of lithium-ion batteries (LiB) have approached their limit regarding their storage capacity. Based on researchers, theoretical energy density of a LiB is approximately 100 Wh/kg — 200 Wh/kg which can hardly meet the expectation of modern applications that require long lasting duration such as automobile (Peng and Chen, 2009). The theoretical energy densities of metal air batteries are about 3 - 10 folds higher than lithium ion battery, making them the best candidate for new generation of electrical vehicle battery. The high energy densities can be explained from the pair of electrodes. Due to its open system configuration, the cathode undergoes reduction when oxygen is intake direct from the surrounding. The metal anode is highly reactive because they have large atomic radii and low ionization energy, valence electron will be readily release when reacting with another chemical compound.

As shown in Table 2.1, the lithium-air battery recorded the highest energy density of 3463 Wh/kg which is several folds higher than the state-of-art LiB (Zhang et al., 2016). It recorded the highest specific capacity of 1170 Ah/kg among the other metal air batteries. In 1996, K.M. Abraham successfully demonstrated the first rechargeable lithium oxygen battery by placing lithium metal as anode and a carbon based cathode separated by a lithium-ion conductive electrolyte (Abraham, 1993). However, Li-air battery has several shortcomings that needed to be tackle by researchers. Lithium peroxide (Li_2O_2) is produced when oxygen reacts with lithium ions at carbon cathode, the compound will be decomposed to lithium carbonate blocking the porous carbon. This enhances the degradation rate, leading to early failure of the battery.

Besides, cathode required pure oxygen for the reduction reaction, the presence of water vapor in the ambient air may damage the cell deteriorating the performance of the system (Lee et al., 2011). Furthermore, the high price of metallic lithium which cost about USD 160 000 per ton impede the wide implementation on most product as society will opt for more affordable battery. Lithium-air cell still require more research and lab testing as there are still many uncertainties that are yet resolve.

Table 2.1: The properties of different metal-air batteries (Zhang et al., 2016).

| Batteries | Voltage (V) | Theoretical Specific capacity (Ah kg ⁻¹) | Theoretical energy density (Wh kg ⁻¹) | Reaction |
|-----------|-------------|--|---|---|
| Al-air | 2.71 | 1030 | 2791 | $4Al + 3O_2 + 6H_2O \rightarrow 4Al(OH)_3$ |
| Mg-air | 3.09 | 920 | 2843 | $Mg + \frac{1}{2}O_2 + H_2O \rightarrow Mg(OH)_2$ |
| Na-air | 2.27 | 487 | 1105 | $Na + O_2 \leftrightarrow Na_2O_2$ |
| Zn-air | 1.65 | 658 | 1085 | $Zn + \frac{1}{2}O_2 \leftrightarrow ZnOH$ |
| Li-air | 2.96 | 1170 | 3463 | $2Li + O_2 \leftrightarrow Li_2O_2$ |
| K-air | 2.48 | 377 | 935 | $K + O_2 \leftrightarrow KO_2$ |

Some of the metal-air batteries are regarded as rechargeable cell for instance lithium-air, sodium-air, potassium-air and zinc-air (Zhang et al., 2016b). Aluminium and magnesium have also been reported to be rechargeable but at a very limited cyclic ability. The anode plays an important part in the reversible reaction, there are 2 main factors that influence the performance in a rechargeable metal-based battery. When anode reacts with alkaline electrolyte, a layer of passivation called solid electrolyte interphase (SEI) is formed. This film composes of degradation products that is detrimental to the battery because it consumes metal ion and electron. However, this film serves as a protection to by allowing small lithium ion to pass and not electrons preventing further degradation of electrolyte. Researches are still trying to improve the stability of SEI by switching electrolyte. The formation of dendrite is another factor that is

detrimental to the performance of rechargeable metal-air battery. Ions travel from anode to cathode during discharge. When the ions travel back during charging period, their original position was dislocated causing uneven surface which leads to the formation of dendrites. Dendrites will penetrate the membrane separator causing cell degradation and short circuit. Although alloying the metal may help impede the formation of dendrites, it will bring adverse effect on the specific energy of the battery. Recently, researchers found that by increasing the current density to a certain point will cause the dendrite to merge together and smoothen the electrode surface (Wang et al., 2018).

The abundance of sodium, which occupy earth's crust by 2.6 %, is found to be suitable replacement for the high cost lithium. Although the energy density may not be comparable to a lithium-air battery, but it can still deliver much higher than a lithium-ion battery with about 1600 Wh/kg (Yin and Fu, 2017). Several researchers have undergone extensive experiment on sodium-air for its rechargeability, reliability and performance to further improve the cell efficiency (Sun, Yang and Fu, 2012). Khan et al. developed a dual electrolyte, mixture of aqueous and non-aqueous electrolyte, at the cathode and anodes compartment respectively. This has significant improvement on the overpotential, charge-discharge and cycle performance of the sodium-air battery (Khan et al., 2017). Another researcher added a bifunctional catalyst which improve the battery energy efficiency, discharge stability and no sign of degradation in 25 cycles. Due to the huge atomic weight, low redox reaction and low cycle life of sodium proves that it is still not matured enough to be commercialized.

Zinc-air battery, as a primary and a rechargeable air cell, is commercialize due to its high energy density and lower production cost. It is available in niche market and comes in various sizes such as hearing aids, film camera and electric vehicle propulsion (Pei, Wang and Ma, 2014). Zinc has variety of advantages over other metal candidates in terms of low cost, portability, low reversal potential, longer life cycle and offer higher storage capacity than lead acid battery. Currently, research is focused on improving the performance, increase the life cycle, finding better catalyst to provide porous stability and enhance the durability of the battery.

Iron-air flow battery has been invented in the 1970. Due to its abundance amount in the Earth's crust, researchers are motivated by the enhanced incentives to developed robust, moderate-cost, environmentally acceptable and rechargeable iron-air battery (Strauß, Vetter and Von Felde, 2012). The challenges face by the iron-air battery are similar with the other metal-air batteries which is the parasitic reaction at the anode accounting to low performance of the battery. The materials used by the iron displays lower discharge voltage and low number of life cycles.

A new research undergo recently is by utilizing metalloid as anode; the material used is silicon. Silicon-air battery attracts much attention due to its availability to provide high energy density (8470 Wh/kg), besides, being the second most abundant element in earth's crust. Silicon is also environmentally friendly and easy to manage its discharge product. The downside of a silicon-air battery is having high corrosion rate which lower the anodic efficiency and influence the discharge performance and cycle life of the battery (Durmus et al., 2018).

2.4 Development of Aluminium-air battery

Among the aforementioned metal air batteries, aluminium-air battery is still in infancy stage and researchers are still exploring to enhance the battery performance, increase the life span and tackle the self-corrosion issue. Although Al-air battery fall short in terms of the power density compare to lithium-ion battery, it was subjected to numerous research as an alternative energy storage due to its merits such as high-theoretical energy density (2791 Wh/kg) and specific capacity (1030 Ah/kg), stable , light weight, abundance in materials, environmental benignity and recyclable waste product (Liu et al., 2017a). Most chemical properties in Al-air battery fall short to lithium-air battery such as specific capacity, energy density and operating voltage, however, due to formation of dendrites, overpotential and safety issues, researchers have venture into developing alternative metal-air batteries (Nestoridi et al., 2008). Therefore, researchers have opted for the second choice which is aluminium-air battery and has been undergoing extensive research for the past 50 years.

Figure 2.4 illustrates the historical breakthrough data that Al-air battery has achieved for the past 50 years (Liu et al., 2017a). Zaromb was the first

inventor of Al-air battery in 1962 and was quick to be recognised by researchers due to its high theoretical energy density (Zaromb, 1963). Different types of electrolyte serve different purpose. For saline electrolyte, the rate of corrosion is low in anode thus it is great for application that require lower power and high energy such as portable electrical device and briny battery. However, in alkaline electrolyte, the high power was facilitated due to solubility of aluminate ion in alkaline solution and higher conductivity. It was being implemented as an energy storage into variety of applications such as electric vehicles (EV), military communications, unmanned underwater vehicles and unmanned aerial vehicles (UAV). The distance travelled by the electric vehicle has increase up to over 3000 km by using Al-air battery.

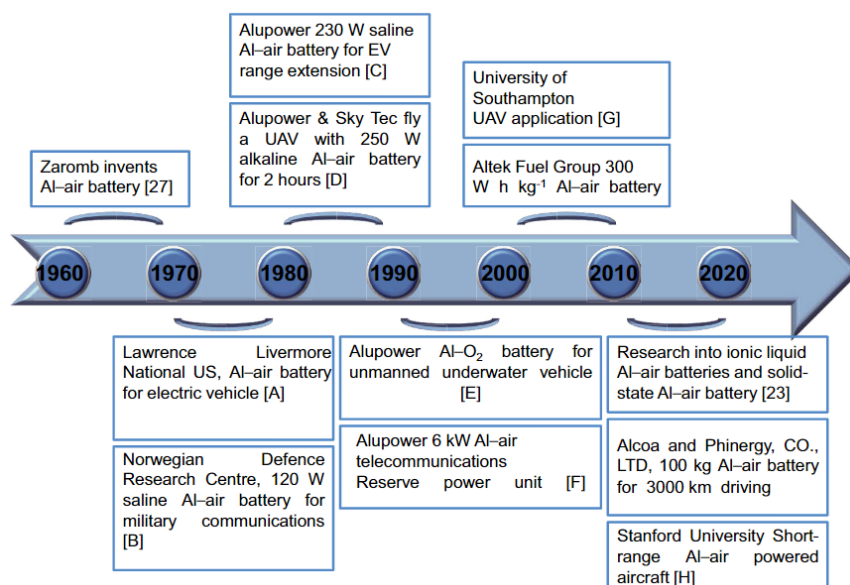
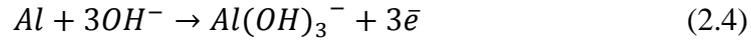


Figure 2.4: Historical development of aluminium air battery (Liu et al., 2017).

Aluminium as a battery anode has generate quite a number of interests among researchers due to presence of tri-valence electron, low atomic mass and high negative standard potential. These properties justified the high theoretical energy density of Al-air battery. Numerous researchers have poured substantial amount of time in amplifying the discharge rate and life cycle of the cell in order for it to be practical to all application.

Al-air battery experiences electrochemical reaction similar to other normal battery, a particular part that distinguish it from other ordinary battery is

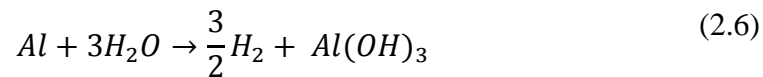
that oxygen is not stored in cathode but instead obtained from the environment to undergo reduction reaction. At the anode, shown in Eq. 2.4, oxidation occurs when aluminium releases electron and turn into aluminate ions.



In Eq. 2.5, a cathode with a carbon-based material is exposed to the environment to absorb oxygen. When electrolyte and catalyst result in an oxygen reduction reaction.



From Eq. 2.6, parasitic hydrogen-generating reaction involve consumption of water and occurs simultaneously with the oxidation of the aluminium; hydrogen gas is released.



Eq. 2.7 shows the overall reaction of the Al-air battery during discharge.



There are two major barriers that hinder the development of Al-air battery from being implemented in large scale mainly the self-corrosion reaction experienced by the aluminium anode and the inefficiency of air cathode. With regards to the challenge of air cathode, many solutions have been come out which include the development of fuel cell technologies and enhancing the materials of the cathode. In addition, researchers have yet to find a perfect solution to overcome the parasitic hydrogen-generating corrosion issue that occurs on the surface of anode. The current efficiency is indirectly proportional to the parasitic reaction contributes to low power output from the cell. Another problem arise is the safety concern due to the accumulation of hydrogen in the

system; explosion may occur. A few solutions have been suggested to overcome the problem such as placing an alloyed aluminium at the anode in order to provide better corrosion resistant, apply different type of electrolyte and modifying the catalyst for the electrolyte.

2.5 Aluminium Alloys

When pure aluminium is inserted in an unmodified alkaline electrolyte, a passive hydroxide layer is formed which cause unstable reaction and inhibits dissolution resulting in overpotential and high corrosion rate from the aluminium anode (Egan et al., 2013). A considerable number of alloying metals have been adopted such as Gallium (Ga), Indium (In), Tin (Sn), Zinc (Zn) and many other metals. Zn element can be found in most aluminium metal. The element has the ability to inhibits hydrogen evolution that is responsible for reducing the amount of hydrogen produced, leading to lower anode degradation. Zn-added anode increases the theoretical battery voltage but severely impact the discharge performance of the metal air battery (Park, Choi and Kim, 2017). When the current flow through the electrode-electrolyte interface, Zn passive film consist mainly of Zn oxide (ZnO) is formed and surrounds the anode surface. This film will slowly inhibit the transfer of ion between aluminium anode and electrolyte leading to decline in battery performance.

In Al-Ga alloy, the chemical reaction is influenced by the weight percent of Ga in aluminium, the temperature of electrolyte and the reactivity of Ga in alkaline electrolyte. In order to intensify the anodic current, at least 0.055 wt% of Ga is preferred at temperature of 25 °C (YU et al., 2015). A much higher mass percent of Ga is required at higher temperature. When being tested in an open circuit experiment, the parasitic reaction is relatively high with no inhibition efficiency. The efficiency of discharge is dependent on the activation of the alloy. Researchers deduce that temperature below 29 °C will cause slow diffusion of aluminium through gallium deposits leading to lesser reduction reaction and corrosion would be less.

In Al-In alloy, the dependant variables on the electrochemistry of the alloy is similar to Al-Ga alloy. At 25 °C, the maximum concentration of In is alloyed at 0.16 % in an aluminium alloy as higher concentration will pose no improvement on the anodic discharge rate. It experiences current fluctuation

because In is not soluble in alkaline electrolyte. Concentrated indiate ion (InO_2^-) will pile up and saturates the active site, however, the ion will dissolve and the oxidation reaction continue takes place after some period. At an elevated temperature of about $60\text{ }^\circ\text{C}$, a lower concentration limit of In will display more chemical reaction leading to higher discharge efficiencies and lower corrosion behaviour.

Other element such as Sn and Manganese (Mn) when alloyed with aluminium are able to enhance the anodic behaviour but also increases the corrosion rate. Researchers are studying the discharge efficiency, current density and electrode potential during discharge of al-air battery if two or more elements are used to alloy aluminium anode. Binary, Ternary and quaternary alloy have been tested in different aqueous alkali solution. Although certain elements are beneficial, other impurities like Iron and Copper are not prefer since they exhibit corrosion in a localize galvanic cell.

2.6 Cathode Electrode

Another essential component in the aluminium air battery system is the air cathode. An air cathode comprises of catalyst layer, current collector and gas diffusion layer. Generally, an efficient air electrode should possess high electrochemical activity for oxygen reduction reaction (ORR), quick migration of OH^- , fast oxygen diffusion rate while prevent water permeating, has stable structure in alkaline condition and good electrochemical conductivity.

Carbon cloth is the most commonly used and applied catalyst support and current collectors in various energy devices. This was mainly due to its economical price with high conductivity and mechanical flexibility. An experiment was done on carbon cloth and carbon paper to compare their performance as gas diffusion electrode of PEMFC (Ma et al., 2014). The experiment results reveal that their physical structure influenced their performance. Under high humidity operations, carbon cloth was able to show higher current distribution. Mass transport limitation was caused by the highly tortuous structure from the carbon paper. However, both of these materials are limited by their smooth surface which makes water-droplet detachment more difficult. Consequently, leading to severe water coverage on the surface and increased mass transport loss.

Carbon fiber are usually combined with other materials to form a composite. When combined with a plastic resin and wound or molded it forms carbon-fiber-reinforced polymer (known as carbon fiber). Carbon fibers are also composited with other materials, such as with graphite to form carbon-carbon composites, which has high heat tolerance. Graphite fibers have carbon contents exceeding 99 % and exhibit high elastic moduli, while carbon fibers have carbon contents between 93 % and 95 % (Jiang et al., 2019). A study was conducted on the electrochemical reduction of Cr (VI) to Cr(III) ions in a dilute synthetic solution using graphite felt (Lakshminathiraj et al., 2008). Graphite felt and carbon felt were preferable for removal of metal ions owing to their high area per unit volume and mass transfer characteristics. The study found that graphite felt outperformed carbon felt at reducing ions. By comparison graphite felt has high electron mobility; it is a good electrical conductor due to occurrence of a free pi (p) electron for each carbon atom, facilitating the transfer of electrolyte ions with air.

2.7 Electrolytes of Aluminium-air battery

Electrolyte act as an essential role in a battery by separating the two electrodes and serve as a catalyst to promote the movement of ions from anode to cathode during discharge cycle and vice versa for charging cycle. The type of electrolyte will influence the properties and performance of the cell. In Al-air battery, aqueous electrolytes are mainly used as it provides higher conductivity to ions. The development on aqueous electrolytes have been focused mainly on two types which are saline and alkaline. Alkaline electrolyte has higher conductivity and higher solubility to regulate hydroxide anions than saline electrolyte (Revel, Audichon and Gonzalez, 2014). Making it suitable for high-power application such as unmanned vehicles, electrical automobile and back-up batteries. However, the corroding process on the anode is detrimental to the metal when reacts with alkaline solution which leads to low current efficiency and shorter battery lifespan. Besides, during battery idling and self-discharge period, Al-air battery could generate unwanted heat causing water loss for the electrolyte and facilitate the parasitic reaction (Patnaik et al., 1994). This pose a potential hazard and unstable reaction that deteriorate the battery life. Research have been

undergone to overcome the obstacles such as implementing a neutral solution and non-aqueous electrolyte.

2.7.1 Alkaline Electrolyte

Researchers are constantly finding ways to operate Al-air battery at higher power density since 1970, but due to technology limitation, passivation of aluminium hydroxide, wearying self-corrosion rate and unsuitable cathode has impeded the commercialization of this battery in large scale. Caustic electrolytes are prominent for its high ionic conductivity, stable reaction at solid electrolyte interface and practical for air cathode. Significant advancement has been made to overcome the corrosion issue in aluminium anode.

Researchers discovered that 7 mol/dm^3 potassium hydroxide (KOH) and 4 mol/dm^3 of sodium hydroxide (NaOH) are favourable to be the alkaline electrolyte of Al-air battery (Egan et al., 2013). The maximum electrolytic conductivity recorded for the former is 0.7 S/cm which surpass the latter which is only 0.39 S/cm . KOH is a cut above NaOH as the former undergoes oxygen reduction reaction more swiftly. Higher diffusion coefficients of oxygen, higher solubility limit of aluminate and lower viscosity makes it more superior than NaOH. However, KOH solution cannot recycle alumina through Hall-Heroult process which will be a concern if implemented for vast production (Linden and Reddy, 2001). Applications that require high power density is preferable to utilize alkaline electrolyte in Al-air batteries:

- Reserve battery. Al-air battery will be placed as a standby battery for lead-acid battery during power disruption.
- Military power unit. It was suitable for military communication device due to its ease of handling, can be activated by water and the heat produce from dissolution of KOH allows the devices to operate at low temperature.
- Unmanned vehicles propulsion. The alkaline aluminium battery is incorporated into unmanned submarine and unmanned aerial vehicle. The battery has the ability to move in long range and produce higher voltage output than fuel cell.

2.7.2 Correlation of electrolyte concentration and battery performance

In an alkaline electrolyte, the current density and the power density are mainly governed by the electrolyte concentration. Researchers experimented on the effects of different concentration of electrolyte on battery performance as display in Figure 2.5 electrolyte (Wang et al., 2013). The open circuit voltage (OCV) varies little with different concentration ranging from 1.45 V to 1.5 V. The short circuit was measured to be 54 to 105 mA/cm² and the peak power density range from 17.5 mW to 36.2 mW / cm² as the concentration increases from 1M to 5M. The deviation of measured open circuit voltage from theoretical (2.7 V) was due to high activation overpotential while the voltage drop during experiment is mainly due to ohmic loss.

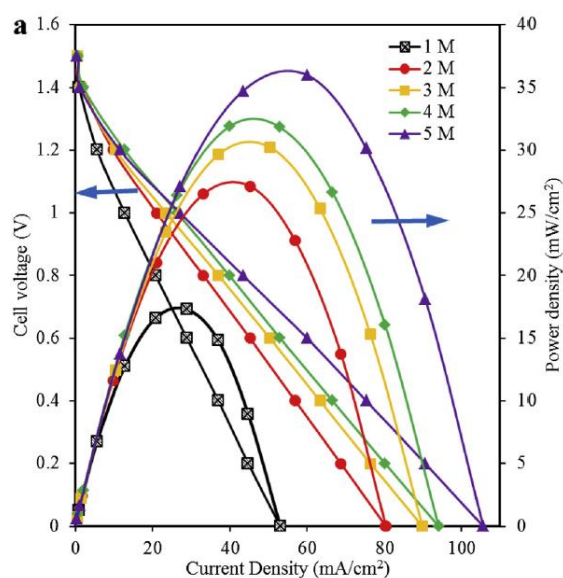


Figure 2.5: The current density, cell voltage and power density with different concentration of electrolyte (Wang et al., 2013).

2.7.3 Inhibitor and Other Types of Electrolyte

Since special formulated alloys needed high-purity aluminium to be supplied, the cost incurred will be relatively high. This has motivated researches to find other means, a cheaper but effective method, to solve the corrosion problem. Researchers found out that modifying the electrolyte by adding inhibitors or additives into the electrolyte is proven to be effective. These inhibitors are typically similar elements that was applied in manufacturing pure aluminium alloy. Stannate ion (SnO_3^{--2}) and Indium hydroxide ($\text{In}(\text{OH})_3$) are able to

enhance the oxidation reaction of aluminium anode as it was found to be successful in suppressing the anode corrosion.

Neutral saline electrolyte is much more preferred due to its lower hazardous system and lower corrosion rate than the alkaline solution. However, the conductivity of aluminium and energy densities is low in a saline electrolyte. Besides, a passive thick oxide layer will form on aluminium and interfere the anodic behaviour and cell polarization. By adding inhibitors, researchers have successfully extend the cell discharge time, improve the power output and the battery efficiency was increase with the decrease in the rate of self-corrosion. A new advancement has been developed to enhance the efficacy of Al-air battery.

A new type of electrolyte, an organic electrolyte, have been adopted in Li-ion battery. By adopting similar concept, the Al was immersed in an organic electrolyte and addition of inhibitor, Na_2SnO_3 , is able to improve the discharge of aluminium (Lucia, 2014). The electrochemical behaviours of Al in organic electrolytes exhibit higher electrochemical reaction with significant reduction of self-corrosion on the anode. Besides, research was done on cotton-based Al-air battery in replacement of its counterpart, paper-based solution. The cotton-based Al-air battery using gel electrolyte stood a better chance in commercializing as it shows 10 times higher power density, higher specific capacity and specific energy than the paper-based Al-air battery (Pan et al., 2019).

2.8 Aluminium as source of hydrogen for fuel cell

The depletion of fossil fuel has led to a significant sales growth for the hydrogen economy as it seems promising as a replacement energy storage due to its environmental benignity. The burning and extraction of fossil fuel leads to environmental pollution, emission of greenhouse gasses and global warming. Innovative ideas have been come up to find a replacement for the conventional combustion of fossil fuel.

Apart from being environmentally friendly, when hydrogen is being utilize by power source such as fuel cell, it can provide sufficient energy to support wide-ranging application for human activities. Currently, hydrogen fuel cell is mainly use in booster rockets in space program by NASA, portable device

that require continuous energy supply, stationary application such as weather station and automobile vehicles. Although hydrogen may seem attractive as fuel alternative in the future, two major issues that faces by this system are the production of hydrogen and the storage location of hydrogen. Researchers are conducting various kind of experiments and tests to overcome the problems. It was reported that 90 % of hydrogen manufacturing process required the combustion of fossil fuel which still bring adverse effect to the environment. Among the present hydrogen produced, 55 - 60 % are produced by natural gas reforming (Buchel, Moretto and Woditsch, 2000). Another hydrogen generation process is through water electrolysis, however, due to the high-priced production process this method is deemed not feasible until more advance technology have been introduced (Jeong and Oh, 2002). An optimum solution for hydrogen storage is yet to emerge as the constraint can't be met. The three main issues are the safety issue of handling hydrogen gas, a huge capacity for storing hydrogen and the resupply of hydrogen.

Researchers came up with the idea of utilizing the generated hydrogen directly from ammonia, hydrolysis of chemical hydrides, and parasitic reaction of Al-air battery immediately which could eliminate the needs of hydrogen storage. Among these approaches, the hydrolysis of aluminium incorporate with the hydrogen fuel cell is the optimal solution for its cost effective, low safety issue and eco-friendly product reaction.

Aluminium is well known for its high discharge current capacity, open-circuit potential and high energy density (Soler et al., 2007). At the anode, when aluminium reacts with an aqueous electrolyte, aluminium hydroxide and hydrogen is produced while the surface of anode is being corroded as shown in Eq. 2.6.

The parasitic reaction is regarded as unpleasant occurrence in Al-air battery as the electron produced from anodic reaction will be consumed by hydrogen via hydrogen evolution reaction (HER). In this study, instead of limiting the parasitic reaction, the hydrogen gas produced will be utilized for the in situ fuel cell. Research conducted an experiment using an aluminium soft drink cans that were submerged in aqueous sodium hydroxide (NaOH) solution while utilizing the supplied hydrogen to a commercial proton-exchange

membrane fuel cell (Marcilio, Tessaro and Gerchmann, 2012). The equation is given as Eq. 2.8.



The polarization data obtained in this study can be clarify based on the electron flow using energy perspective, in Figure 2.6 (Yang and Knickle, 2002). When reaction occurs, electrons released have two flow paths. The main path is the aluminium/air sub-cell ($\text{Al}/\text{Al}(\text{OH})^-$) where the electrons flow from the aluminium anode to the gas diffusion cathode. The alternative path would be through hydrogen anode ($\text{H}_2/\text{H}_2\text{O}$) to the gas diffusion cathode, electrons in Al would initially drop to $\text{H}_2/\text{H}_2\text{O}$ with certain energy loss due to parasitic reaction and subsequently flow from hydrogen anode to cathode. Overall, the electron flow from high energy level $\text{Al}/\text{Al}(\text{OH})^-$ to lower energy level O_2/OH^- . Instead of dissipating H_2 as exhaust it reutilizes it for electricity generation through the hydrogen/air sub-cell.

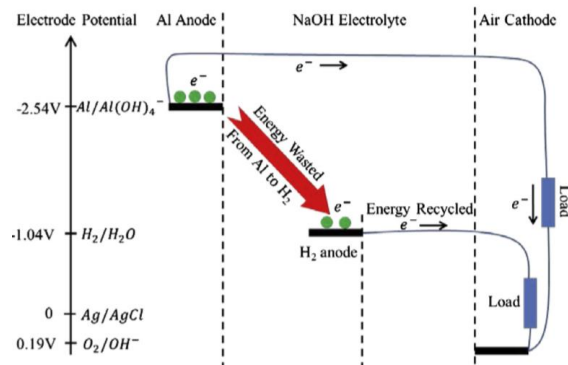


Figure 2.6: Working principle of the hybrid system from energy view point (Yang and Knickle, 2002).

CHAPTER 3

METHODOLOGY AND WORK PLAN

3.1 Introduction

This section presents about the procedures and steps needed to be taken to achieve the aim and objectives of this research, readers will be clearly notified on the purpose of approach taken regarding the experiment. In the electrochemical reaction of aluminium-air battery, apart from the anodic and cathodic reaction occurred as stated in equation 2.3 and 2.4, the present of parasitic reaction has resulted in the production of hydrogen gas. A novel approached has been suggested to overcome the adverse parasitic reaction into a beneficial process. A tandem cell design and construction of aluminium air battery and fuel cell is being proposed. In the experiment, the hydrogen gas produced from the self-corrosion reaction will be utilized by the hydrogen/air sub-cell. This experiment will be cost effective as it eliminates the usage of aluminium alloy and corrosion inhibitors. A structured manner work plan is being established, in order to review the progress of the research. Information gathered from literature review will be use to design and construct the aluminium air-battery fuel cell prototype. The flow chart shown in Figure 3.1 will act as a guidance to conduct this research.

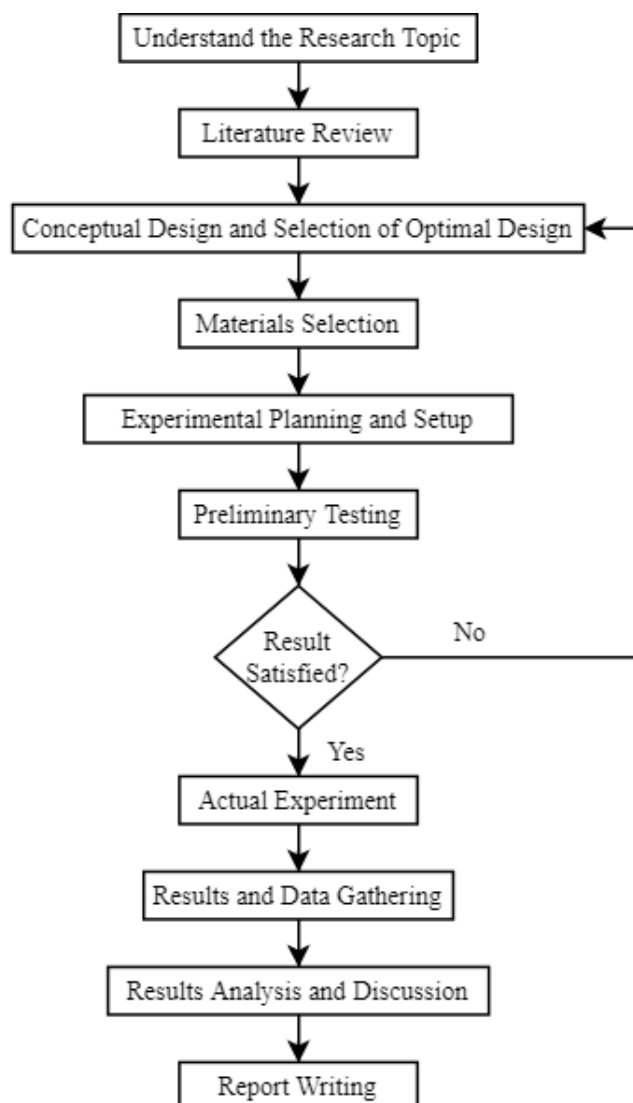


Figure 3.1: Work Flowchart

3.2 Design of Prototype

The tandem cell system comprises of 2 sub-cells: aluminium-air sub-cell and hydrogen-air sub-cell. The aluminium-air sub-cell is made up of aluminium anode and carbon cloth air cathode whereas the hydrogen-air sub-cell use hydrogen anode and share the same cathode with aluminium-air sub cell.

The aluminium will be placed at the bottom of the test rig, allowing the hydrogen gas float towards the carbon cathode and hydrogen anode. A space separating the anode and cathode is filled with electrolyte; the medium that starts the electrochemical process and transport moving ions released by the electrodes. The first conceptual design, shown in Appendix A-1, was not chosen

because the cathode from both sub-cells can be combine into one. Besides, the design is much more complicated to place the hydrogen storage in the middle of the system. Thus, the hydrogen compartment is shifted to the top. The finalised design of prototype was drawn using Solidworks. Figure 3.2 shows the design and cross-sectional area of the prototype cell.

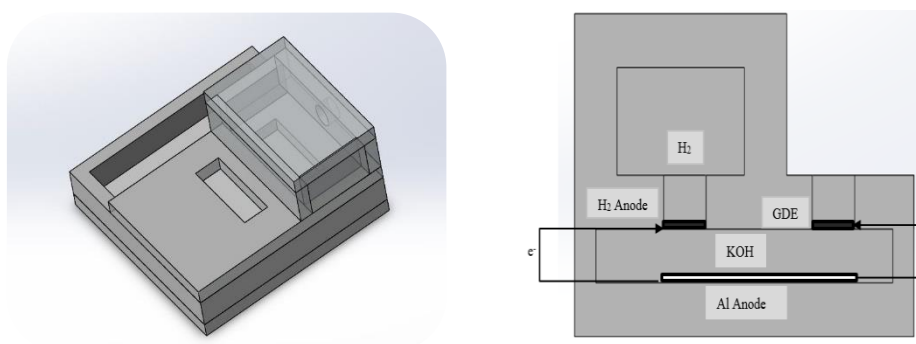


Figure 3.2: Prototype Design (left) Cross-section Area of Hybrid Cell (right)

3.3 Materials Preparation

Aluminium-air battery fuel cell hybrid comprises of 5 main components: anode electrode, air cathode, electrolyte, hydrogen anode and the battery structure body. The 1M of aqueous potassium hydroxide electrolyte was prepared by dissolving KOH pallets in a beaker with distilled water. KOH is preferred because it exhibits higher ionic conductivity than Sodium Hydroxide.

The anode used was household aluminium foil (Reynolds Consumer Products LLC) that is used for wrapping consumable products. The foil contains inferior quality aluminium, the composition of this product will be analysed by Scanning Electron Microscope (SEM) to detect the presence of impurities. The aluminium foil will be measured and cut similarly according to a specific dimension throughout the whole experiment so that it will not affects the result. It will be folded in several layers up to ensure that the aluminium is enough throughout the experiment.

The air cathode and hydrogen anode used were carbon cloth, for preliminary test. The battery casing will accommodate the electrodes and electrolyte. An outlet of hydrogen was constructed and attached with hose barb to verify the gas produced is hydrogen gas. The experiment was conducted at ambient temperature and 1 atmospheric pressure.

3.4 System Fabrication

The hybrid aluminium air fuel cell system composed of 4 parts: an aluminium air sub-cell, battery casing, hydrogen collection compartment and hydrogen air sub-cell.

The battery casing is made of polymethylmethacrylate, or Perspex, sheets with thickness of 5 mm and are combined to form a container. Figure 3.4 shows the prototype of the hybrid system. The dimension of the battery case is 80 mm x 80 mm x 15 mm according to length, width and height respectively. The Perspex were sliced by using a laser cutter, in Figure 3.3. 5 sheets of PMMA were used as the base of the casing. 2 holes with dimension of 3 cm x 1 cm were made to house the cathode electrode and hydrogen anode. 4 holes with diameter of 1mm were drilled around them as copper wire will be used to fix the position of the carbon cloth and hydrogen anode.



Figure 3.3: Laser cutter machine for slicing Perspex glass.

The sheets were joined by using acrylic glue via the process called solvent welding. The applicator is directed at the side of the sheet and adequate pressure is applied onto it so that sufficient amount of glue is used to stick the sheets. The sheets were press against at a fixed position by a heavier object for few minutes in order to maintain the desired shape. Silicon sealant was applied at the joint to prevent leakage of electrolyte. The depth of the base is 10 mm to separate the GDE and aluminium, besides, allowing electrolyte to flow between

them. A compartment for hydrogen gas was built on top of hydrogen anode in order to contain excess hydrogen gas. A hole was made to retrieve hydrogen gas, using the hydrogen collector as shown in Figure 3.4. Hose barb is inserted into the hole.

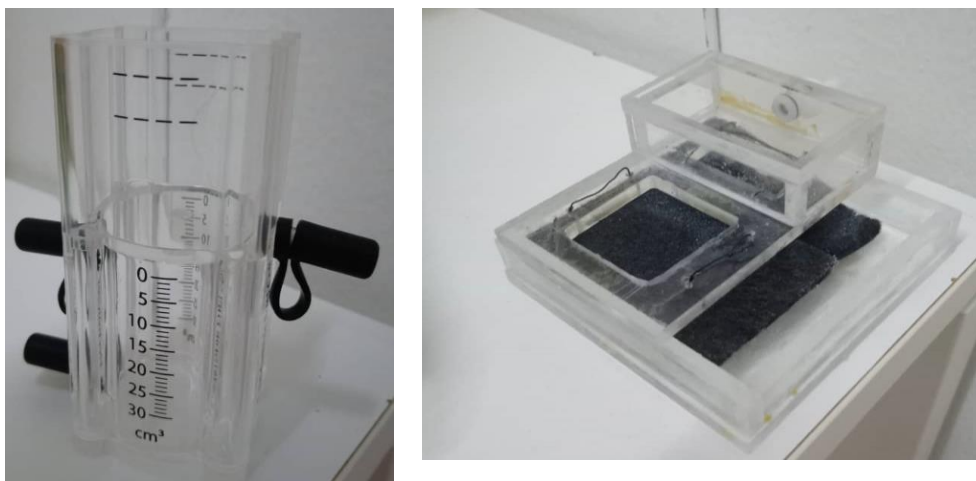


Figure 3.4: Hydrogen collector (left) Prototype of aluminium-air battery fuel-cell (right).

3.5 Preliminary Test

To ensure the feasibility of study, a preliminary testing was conducted to ensure that the testing methods are correct. The cell performance test was carried out using ZIVE SP1 Potentiostat/Galvanostat workstation. Two different types of tests were performed on each couple cell: the aluminium-carbon cloth (Al/air) sub-cell and the hydrogen-carbon cloth (H_2 /air) sub-cell.

Two-electrode configuration was used for the first cell performance test. Al/air sub cell will be connected to the work station as shown in Figure 3.5. The working electrode (red clipper) is connected to aluminium while the counter electrode (black clip) is connected to the gas cathode. The technique used is linear sweep voltammetry (LSV), and the parameters were set to include a scan rate of 10mV/s and a scan range from the open circuit voltage to 0V. The size of aluminium foil used is 6cm x 6cm throughout the whole experiment. After setting up KOH electrolyte was poured into the test rig from the inlet.



Figure 3.5: Experiment Setup for Performance Test. Connection from Work Station to the Al/air Sub-cell.

For the second test, single electrode polarization test, Al/air sub cell was tested using three-electrode configuration with an addition of silver/silver chloride electrode (Ag/AgCl) as reference electrode; set up as shown in Figure 3.6. The working electrode is point of interest as it is the electrode that is being monitored. For example, when aluminium is being examined it is connected to the working electrode while the carbon cloth is connected to the counter electrode. The position is swapped when carbon is the point of interest. For the hydrogen/air sub-cell test, aluminium foil will be placed into the test rig to produce hydrogen gas that will be utilized by hydrogen anode.

The setup was different as the reference electrode cannot be accommodated in the hybrid test rig. In order to analyse the results, the potentiostat/galvanostat data for current and potential value was exported to Microsoft Excel spreadsheet and plotted to create each tests' corresponding polarization curve (I-V curve). Similar procedures and testing methods were carried for the H₂/air sub-cell, by replacing the connection for aluminium anode to hydrogen anode.

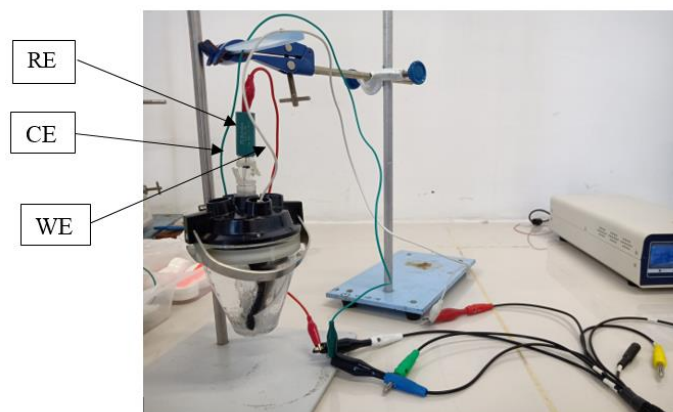


Figure 3.6: Carbon Cloth Single Electrode Polarization Test Setup. Reference Electrode (RE), Counter Electrode (CE) and Working Electrode (WE) was connected to Ag/AgCl, Aluminium and Carbon Cloth respectively.

3.6 Optimization Test

After analysing the results obtained, a few modifications were done to improve the system performance. One of the changes made were replacing the material of air cathode and hydrogen anode from carbon cloth to graphite felt. Another modification made was increasing the dimension of air cathode from 1.5 cm x 1 cm to 3 cm to 1 cm, which allows more air to be absorbed and further facilitate the exchange of ions. Similar performance cell test and experiment setup as shown in Figure 3.4 and 3.5 from Section 3.6 were run, the results were compared and plotted in Chapter 4.

3.7 Verification of Hydrogen Gas Test

The aluminium was placed inside the test rig and electrolyte was poured into it. The reaction was left to run for 10 minutes to let the electrolyte to be saturated with dissolved hydrogen and allowing the hydrogen gas compartment to be filled with hydrogen gas. A splint is lit and held near the hose barb, then the seal is removed to expose the splint to the gas. The splint was also placed near the bubbles that were floated onto the surface of the electrolyte. If hydrogen gas is present, a pop sound will be produced.

3.8 Aluminium Utilization Test

The apparatus was set up, depicted in Figure 3.7, to measure the utilization efficiency of aluminium and evolution rate of hydrogen. 4 different concentration of KOH electrolytes were prepared: 1M, 2M, 3M and 4M. A hole at the hydrogen anode was cut open allowing gas to flow into the hydrogen collector. The hydrogen collector was filled with water until a certain level. The hydrogen gas will enter the compartment through the plastic tube while water will seep out of the compartment as hydrogen gas occupy the space; the drop in water level is recorded. The aluminium was place at the bottom followed by the loading of electrolyte and was left to run at open circuit voltage for few minutes to dissolve the aluminium oxide layer. Parafilm was used to seal the electrolyte inlet to avoid hydrogen gas from escaping to surrounding. Each data was obtained point-by-point by measuring the current potentiostatically. The cell voltage will be manipulated by changing the value of current, for example, when the current is set at 4 mA the voltage output is 1.2 V. The amount of hydrogen gas generated will be collected and measure in the hydrogen collector. the Hydrogen generation rate-voltage curve is plotted, the hydrogen generation rate was measured in unit of $\mu\text{L/s}$. The mass of aluminium was weighed prior to and following of experiment to calculate the amount of aluminium that has been consumed in the reaction. It is then used to calculate the utilization efficiency for aluminium. The results were calculated and plotted in aluminium utilization efficiency-voltage curve.

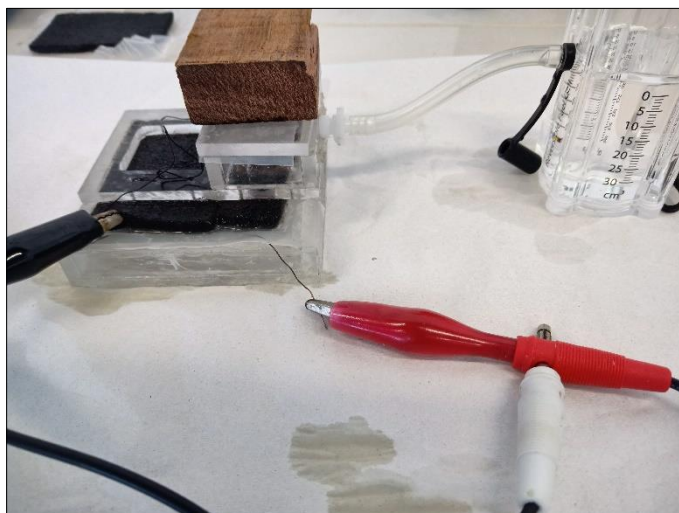


Figure 3.7: Efficiency Testing Setup. The test rig was connected to the hydrogen collector by the plastic tube.

3.9 Performance on Optimised Cell Test

Performance on Optimised Cell Test was done using 2-electrodes configuration similarly as Section 3.5 but with 4 different concentration of electrolytes: 1M, 2M, 4M and 5M. The results obtained were measured and plotted. The real efficiency of the hybrid system was calculated by corresponding the data obtained from aluminium utilization test and polarization curve of optimised cell. The efficiency was calculated for different electrolytes and the results were tabulated in Chapter 4. The discharge test for aluminium air cell is carried out to determine the cell's capacity. The testing time for is 1 hour, 4M of potassium hydroxide is used as electrolyte and the mass of the aluminium was recorded before and after the experiment. The discharge current is set at 10 mA, 20 mA and 50 mA, the results are recorded and plotted.

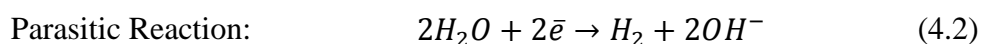
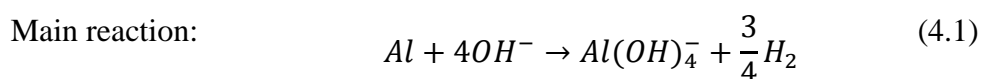
CHAPTER 4

RESULTS AND DISCUSSION

4.1 Introduction

The results and discussion from this chapter is sectioned into four major parts namely the preliminary cell performance test, gas collection test for aluminium utilization test, optimized performance test and system efficiency testing. 2 types of preliminary cell performance test were performed namely the 2-electrodes configuration cell test and single electrode cell test. Different concentration of electrolyte was used to test the efficiency and overall performance of the hybrid system to study its feasibility in various real lives application. The results recorded will be graphically presented for ease of comprehension and explanation. Discussion were included to justify the results obtained or error occurred from the experiment.

Figure 4.1 display the schematic model for the electrochemical reaction of the hybrid cell. The reaction can be decomposed into two reaction: the main reaction and the parasitic water reduction reaction. The main reaction involves the hydroxide ions (OH^-) from potassium hydroxide reacting with aluminium anode, producing Aluminium hydroxide ($\text{Al}(\text{OH})_2^-$) and electron. The parasitic reaction will consume some electron and decompose water to produce hydrogen gas (H_2) and OH^- . The hydrogen gas was utilized by the in situ hydrogen anode. Eq.1 and Eq.2 respectively represent the main reaction and parasitic water reduction reaction that occurs at the surface of aluminium.



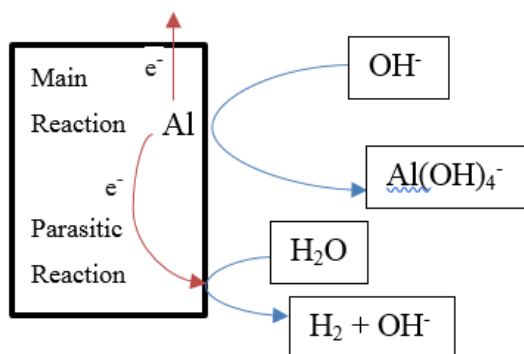


Figure 4.1: Electrochemical reaction of aluminium in alkaline solution.

4.2 Preliminary Test

4.2.1 Performance of Aluminium/air Sub-cell

Figure 4.2 displays the polarization curve for the Al/air sub cell. The cell is recorded to have an open circuit voltage (OCV) of 1.33 V and short circuit of approximately 28 mA. The maximum power output was recorded to be 6.20 mW when the current output was approximately at 15 mA. The cell experienced rapid voltage drop until 5 mA due to activation loss. Subsequent polarization data obtained shows that the voltage drop is proportional to the current output. This is due to the fact that internal resistance increases as current increases, otherwise known as ohmic loss.

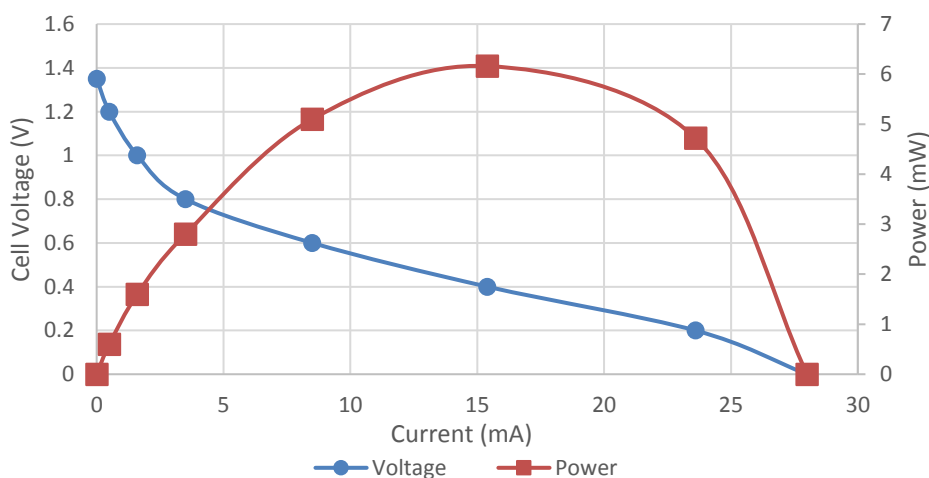
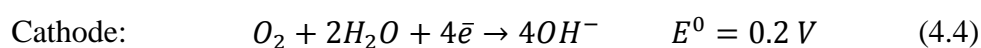


Figure 4.2: Polarization Curve of Aluminium/air Sub-cell.

4.2.2 Hydrogen/air Sub-cell Performance

To further validate the results obtained, single electrode polarization was conducted for both electrodes separately as shown in Figure 4.3. The standard potential of aluminium and carbon cloth against silver/ silver chloride (Ag/AgCl) as reference electrode were plotted at -2.5 V and 0.2 V respectively. From experiment, the potential of Al changes linearly from -1.33 V to -0.62 V, a larger negative value signifies that oxidation is more likely to take place at this half-cell. The decrease in voltage is due to the decreasing activity of OH⁻ ions. Contrary to expectation, the measured standard potential of aluminium is significantly different from the theoretical standard value. The OCV was recorded to be -1.33 V as oppose to the theoretical value of -2.51 V, bringing a huge gap of 1.18 V. The drop in voltage is called overpotential. This may be attributed from the parasitic reaction and activation loss that occur in aluminium when it reacts in aqueous alkaline electrolyte.

Activation loss in this sub-cell presumably due to the blockage of Al₂O₃ that forms on the surface of aluminium. Carbon cloth decreases linearly from -0.20 V to -0.62 V. One of the plausible explanations for the deviation of value from theoretical standard potential is due to the absence of good oxygen reduction electrocatalyst such as platinum on the carbon cloth (Wang et al., 2013). Pristine carbon cloth has pore diameter of 10 μm with several tens of these forms between the structure offering abundant electrolyte transport pathways. However, with high porosity and large pore size has decreases the proportion of carbon cloth, leading to low specific surface area, poor catalytic activity and limiting the battery performance (Zhao et al., 2018). The aluminium anode and carbon cloth cathode reaction is shown in Eq. 4.1 and Eq. 4.2 with their respective standard electrode potential:



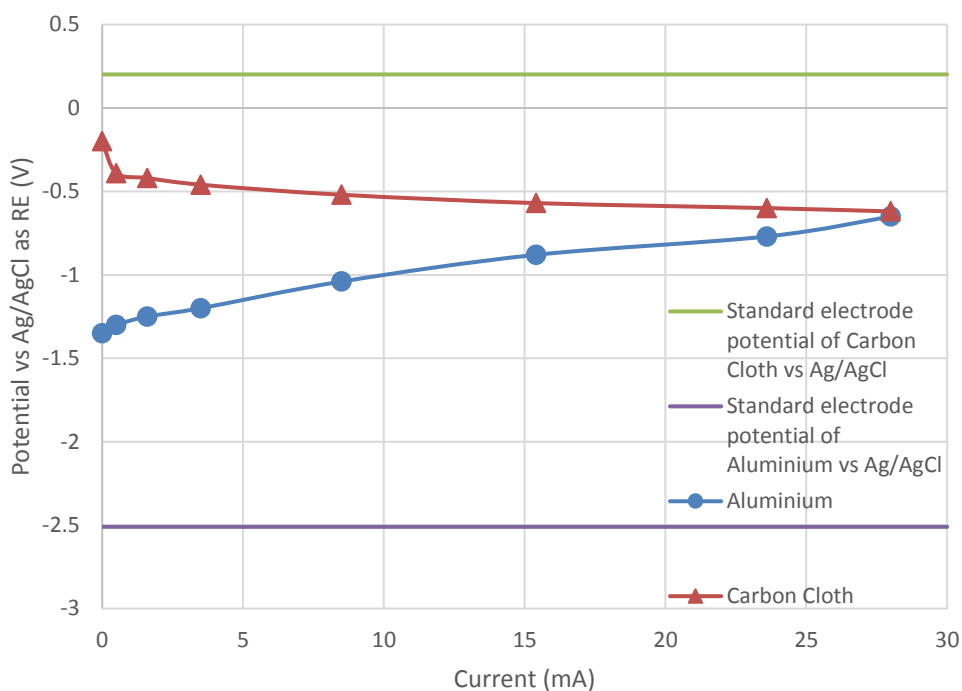
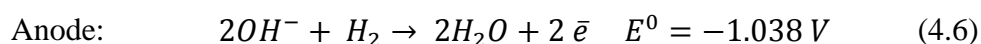
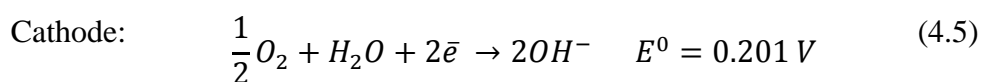


Figure 4.3: Single electrode polarization data of Aluminium/air Sub-cell.

For the hydrogen/air sub-cell, reaction initiates at the cathode side in which the oxygen will be reduced to OH^- by a portion of electron produced from the main reaction. Subsequently, the OH^- produced and the hydrogen gas produced by the parasitic water reduction shown in Eq. 4.2 are utilized by the hydrogen anode that is stationed in the system. The standard electrode potential for the cathodic and anodic reactions taking Ag/AgCl as reference electrode are presented in Eq. 4.5 and Eq. 4.6 respectively.



The polarization curve of hydrogen/air was constructed as shown in Figure 4.4. The cell displays almost a linear polarization curve with V_o of 0.8 V and short circuit current of 15 mA. The measurement of polarization experienced some disturbance that was probably caused by the inconsistent H_2 bubbles generated from the aluminium anode. The peak power recorded was 2.73 mW when current is discharged at 9.1 mA.

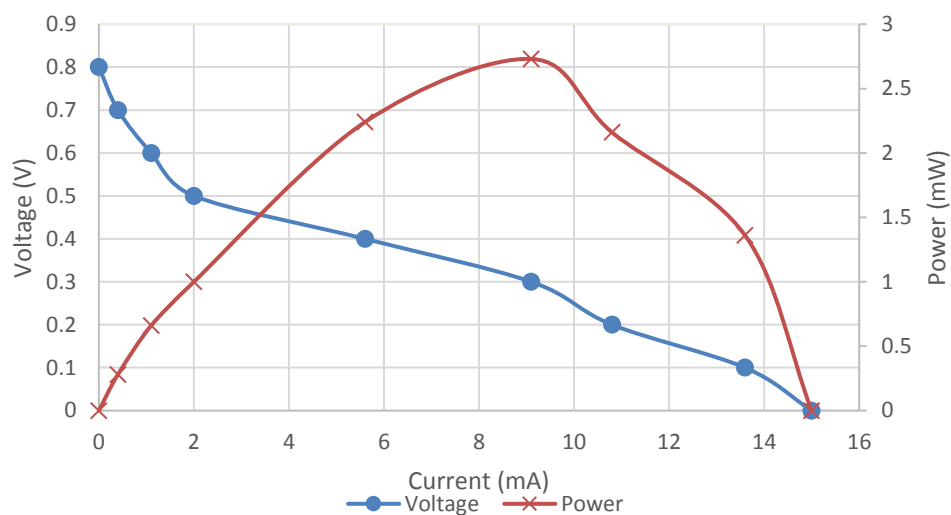


Figure 4.4: Polarization Curve of Hydrogen/air Sub-cell.

Single electrode characterization experiment was carried out similarly as previous sub-cell and the result was plotted as shown in Figure 4.5. The deviation from theoretical standard potential was significant for both electrodes, the anode and cathode experiences quite some activation loss at approximately 0.2 V and 0.4 V respectively against the standard electrode potential. The potential of anode decreases from -0.8 V to -0.44 V while cathode reduces from -0.2 V to -0.44 V.

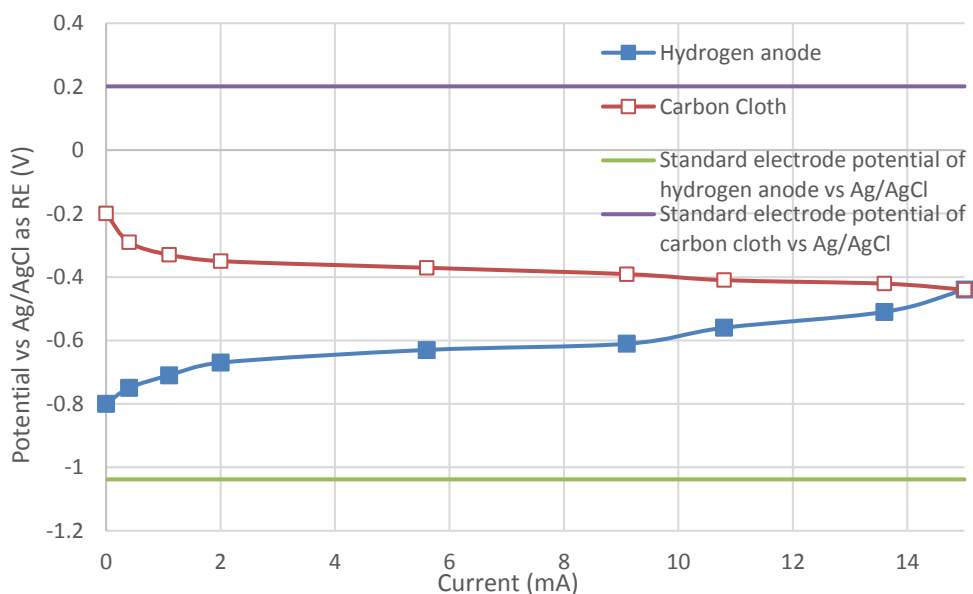


Figure 4.5: Single Electrode Polarization Data of Hydrogen anode/air Sub-cell measure vs Ag/AgCl as Reference Electrode.

Considering the peak power output from Figure 4.1 and Figure 4.3, with the addition of hydrogen/air sub cell the whole tandem cell achieved an increase of power output by 44 % from 6.20 mW to 8.93 mW.

Thereinafter mentioned is the discussion regarding the results obtain on the performance graphs. The polarization curve can be divided into 3 region and the voltage drop in each region derive from different loss. Figure 4.1 is separated into their respective area and portrait in Figure 4.6. From the voltage output graph in Figure 4.6, the first region is called activation loss region. A large drop of voltage can be seen when the load is low. This is the kinetic loss due to very slow reaction kinetic of oxygen reduction in the cathode side. This in turn requires a large overpotential (voltage loss) to drive any practical current density. Researchers found that by coating a layer of platinum catalyst on the air cathode can improve the performance of the system (Jiang et al., 2019).

Region 2 is called Ohmic loss region. This loss is due to presence of internal resistance of the system when current is passing through the cell. Some of the factors that attribute to the loss are the characteristics of electrolyte and electrode and the physical interconnections in the cell. The low molarity of electrolyte with less OH^- and the spacing between the anode and cathode may contribute to Ohmic loss. At the aluminium/air sub cell, the formation of hydrogen bubble and Al_2O_3 block the contact between the electrolyte and electrodes. Besides, hydrogen gas can be seen attaching on the surface of aluminium since it cannot deplete fully, resulting in the increase of internal resistance (Zhang, Klasky and Letellier, 2009). The energy loss from internal resistance is in the form of heat.

Region 3 shows a quick drop of voltage due to mass transport losses. Mass transport loss usually occurs at high current density due to reactants cannot be delivered to the catalyst active site quickly enough, due to the low porosity of the electrode or water flooding or residue from the corroded aluminium foil that prevents the reactant flow. Some suggestions have been came up to reduce these losses such as using a larger surface area of electrode, increase the concentration of electrolyte and use a lower resistivity electrode (Liu et al., 2013).

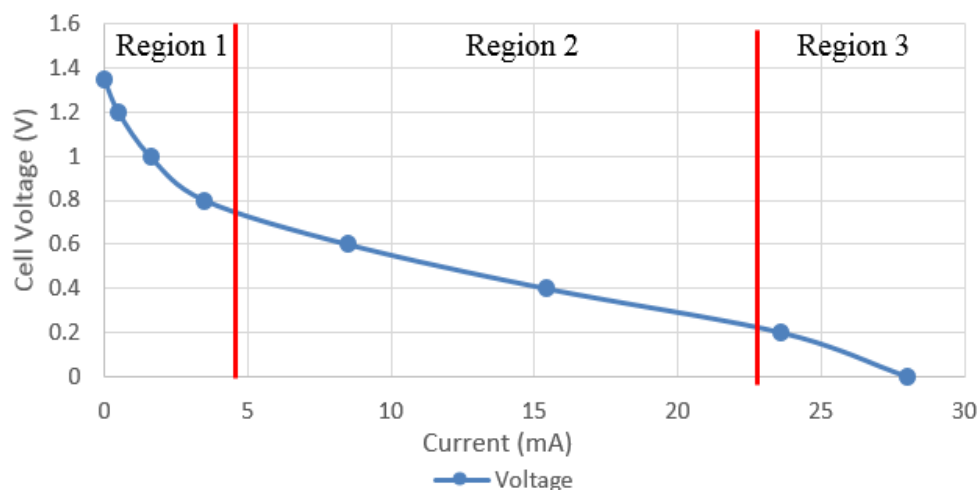
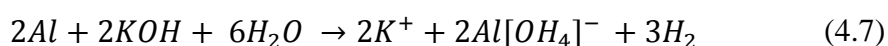


Figure 4.6: The Polarization Curve Classified into Respective Loss.

4.3 Hydrogen gas test

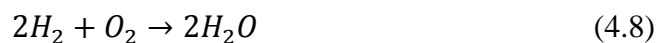
To ensure the feasibility of using the gaseous by-product from aluminium/air sub cell, the burning splint test was employed. When the burning splint was placed near the gas outlet, a faint squeaking sound can be heard. To further validate the result, another test was done at the electrolyte inlet where gas bubbles was seen floating to the surface. When the bubbles were popped with the lit splint, a louder pop sound and a larger flame were produced. From the 'pop' sound, it can be deduced that hydrogen gas was contained in the bubbles. A plausible explanation that the sound was not visible when tested at the hose barb was because there's ambient air in the hydrogen compartment.

When aluminium reacts with potassium hydroxide, hydrogen is produced, this can adequately explain with Eq. 4.7.



The system was left run for some time in order to allow hydrogen to fill the gas compartment. Due to the presence of un-reactive aluminium oxide on the surface of aluminium, the reaction takes a longer time to get going. Thus, the oxide layer will need to be broken down first for the aluminium to react.

The production of bubbles was due to the reaction of hydrogen and oxygen as shown in Eq.4.8. The swift reaction resulted in many bubbles are produced and large amount of energy are dissipated.



4.4 Optimization

Based on cell performance test in Section 4.1, some modifications were done to improve the performance of the hybrid cell. In order to reduce the high activation loss and ohmic loss, the surface area of gas diffusion electrode as well as the cathode material used were improved which was assumed to be the root cause of poor performance from the hybrid cell.

4.4.1 Optimization on the type of electrodes

The contact area of cathode electrode was increased from 1.5 cm x 1 cm to 3 cm x 1 cm as it is likely that the small surface area has causes a limitation on the cell ability to undergo oxygen reduction reaction. The material of the cathode was changed from carbon cloth to graphite felt.

From the single electrode characterization in Figure 4.2 and Figure 4.4, a notable drop in voltage can be seen initially when current is applied. This overpotential was mainly due to activation lose. Thus, in order to improve the performance of the system, carbon cathodes were substitute with graphite felts and were integrated into the system. Figure 4.7 and Figure 4.8 shows the polarization curve and single electrode characterization curve using two different cathode material namely carbon cloth and graphite felt the they were differentiated as previous and new respectively.

From Figure 4.7, the activation overpotential loss is decreased considerably. The deduction is based on the initial voltage drop that occurs from 0 mA to 5 mA. The voltage loss from carbon cloth plummets to 0.7 V from OCV of 1.33 V while the voltage drop by graphite felt is comparatively low from 1.4 V to 1.1 V. The short circuit current for graphite felt is 40 mA and achieved a boost in the maximum power output from 6.20 mW to 13.8 mW. From Figure 4.8, the aluminium experiences steady voltage drop from 1.4 V to -0.65 V. Graphite felt has a smaller activation loss of 0.2 V than carbon cloth; while voltage was dropping progressively until -0.65 V.

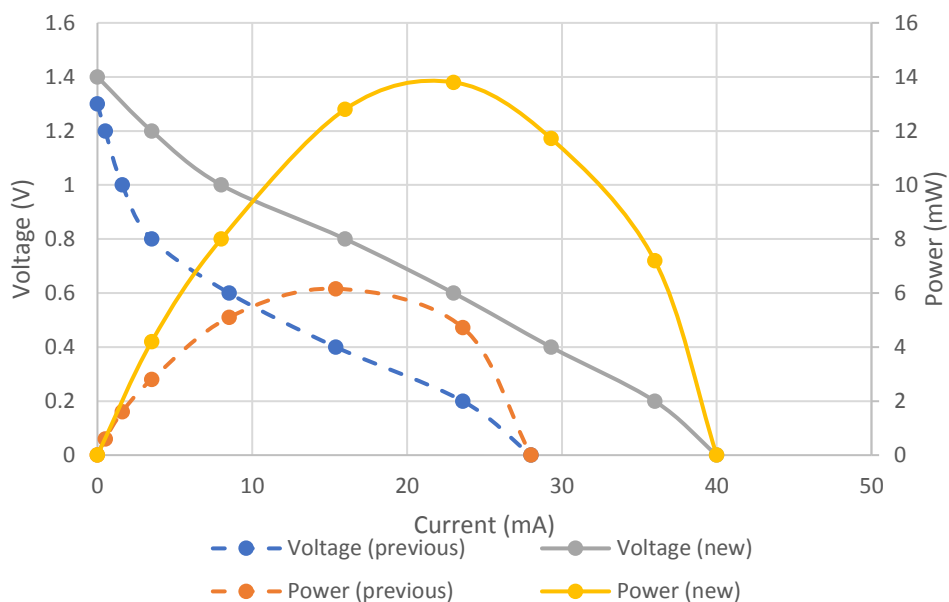


Figure 4.7: Polarization Curve between Carbon cloth(previous) and Graphite(new) at Aluminium/air Sub-cell.

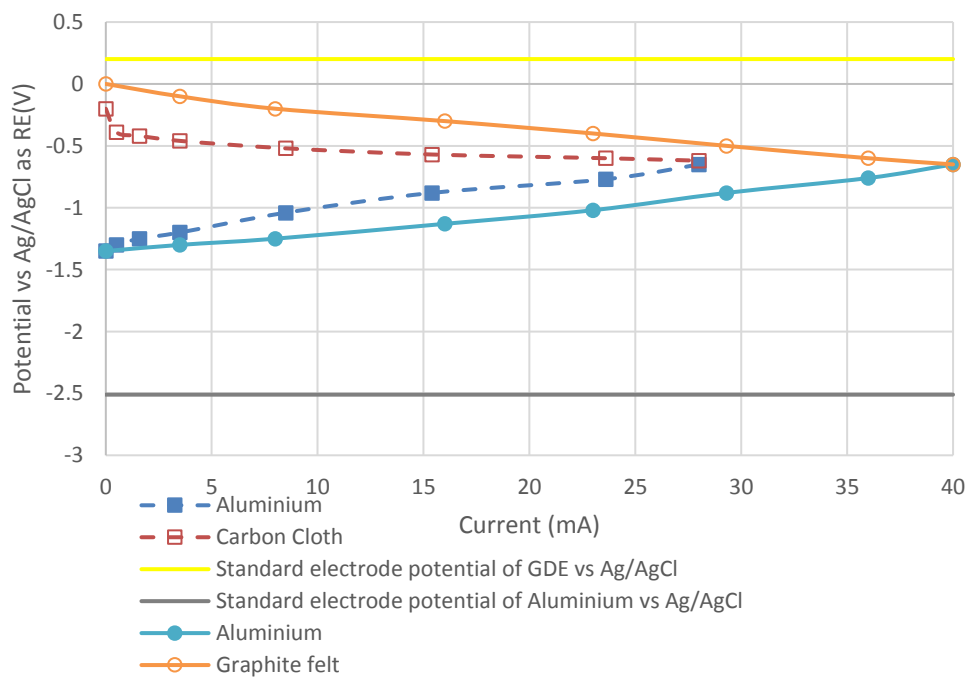


Figure 4.8: Standard Electrode Polarization Data between Carbon Cloth (dashed line) and Graphite Felt at Aluminium/air Sub-cell.

Likewise, from Figure 4.9, the graphite felt is able to outperform its counterpart carbon cloth at hydrogen/air sub-cell. The OCV was recorded at 1 V and short circuit of 23 mA. This cell was able to achieve a higher maximum power of 5.80 mW; 3.07 mW higher than carbon cloth. At Figure 4.10, both the hydrogen anode and graphite cathode are able to reduce the system activation loss. The hydrogen anode achieved an activation loss of only 0.038 V while for graphite cathode is 0.2 V. The hydrogen anode decreases from -1 V to -0.4 V while graphite felt decreases from 0 V to -0.4 V.

Combining both cells together, the optimised hybrid system was recorded to have a maximum power output of 19.6 mW, about 42 % increased with the embodiment of hydrogen/air sub-cell. By operating with graphite, the whole system was able to increase power by 10.67 mW with respect to using carbon cloth.

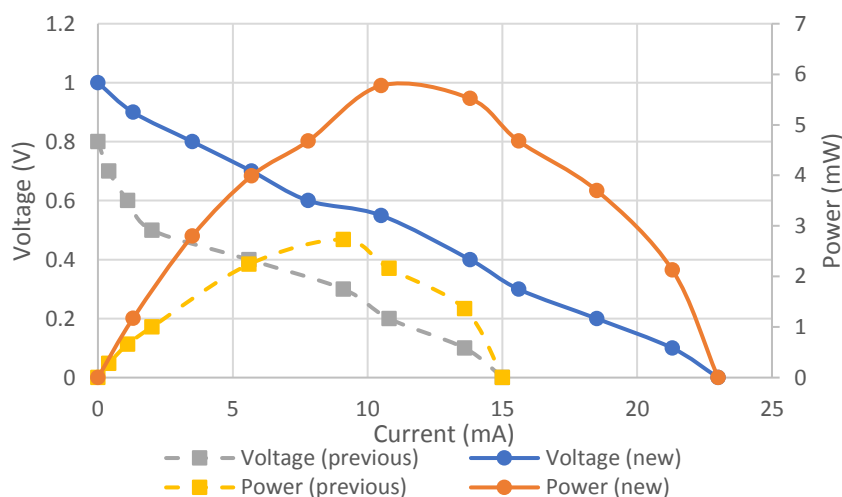


Figure 4.9: Polarization Curve between Carbon cloth(previous) and Graphite(new) at Hydrogen/air Sub-cell.

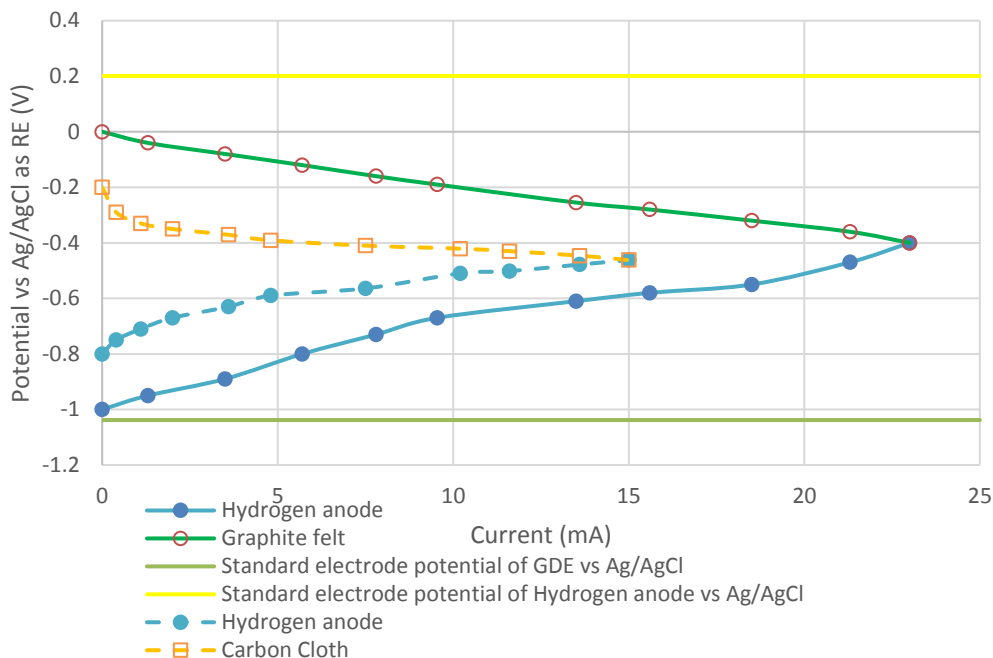


Figure 4.10: Standard Electrode Polarization Data between Carbon Cloth (dashed line) and Graphite Felt at Hydrogen/air Sub-cell.

As mentioned in Chapter 2, graphite felt outperforms carbon cloth is attributed from its' thicker dimension that leads to larger surface area for reactant to undergo reduction. The large pore graphite felt with its' interlace fibers structure, allows easier access of oxygen through the felt further facilitating reactant transport and reduces cell resistance (Pounce, 2007). Besides, graphite has good electrical conductivity attributed from its high permeability. On the other hand, the tortuous structure of carbon cloth contribute to the severe mass transport limitation. The smooth surface was detrimental to the performance of the system as it makes water droplet detachment difficult, hindering the exchange of oxygen with electrolyte ions. Consequently, leading to severe water coverage on the surface and increased mass transport loss.

4.5 Aluminium Utilization Test

The utilization test of aluminium was carried out and the required information for calculating efficiency was recorded in Table 4.1. Aluminium utilization efficiency was calculated using Equation 4.9. When the aluminium undergoes oxidation, electrons are released for the main reaction to generate electricity

while hydrogen from the parasitic reaction will be used for hydrogen anode. The aluminium utilization efficiency (ϵ) is calculated using Eq. 4.9.

$$\epsilon = 1 - \frac{\text{amount of Al consumed in parasitic reaction}}{\text{total amount of Al used}} \quad (4.9)$$

The utilization efficiency is highly dependent on the aluminium working potential and the electrolyte concentration. The amount of aluminium consumed in parasitic reaction is calculated from the amount of hydrogen gas produced. Therefore, the aluminium utilization efficiency depends on the amount of hydrogen gas released. Thus, the ratio of the main reaction to parasitic reaction is $\epsilon: (1 - \epsilon)$.

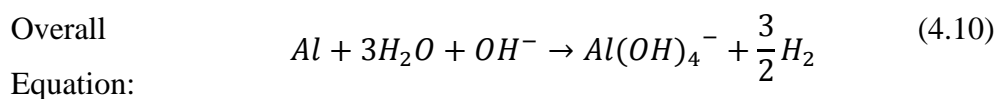
Thereinafter describe the calculation of efficiency by applying 1M to illustrate the testing. The hydrogen gas collected was also used to calculate hydrogen evolution rate(r_H). Hydrogen evolution rate are calculated to observe the amount of hydrogen gas produced when different voltage is being tested. Table 4.1 shows the data recorded for the utilization test at 1M concentration of electrolyte when tested at different voltage.

Table 4.1: Data for Volume of Hydrogen Gas Collected, Mass of Aluminium Used, Hydrogen Generation Rate, and Efficiency at 1M Concentration.

| Voltage | Volume of H ₂ collected (ml) | Mass of Al used (g) | Hydrogen generation rate, r_H ($\mu\text{L/s}$) | Efficiency, ϵ (%) |
|---------|---|---------------------|---|----------------------------|
| 1.3V | 8 | 0.0126 | 4.445 | 50.0 |
| 1.2V | 5 | 0.0102 | 2.778 | 60.7 |
| 1.0V | 2 | 0.0090 | 0.277 | 82.1 |
| 0.7V | 1 | 0.0087 | 0.0556 | 90.8 |
| 0.3V | ~1 | 0.0082 | 0.0556 | 90.2 |

In order to use the efficient equation from Eq. 4.9, the units for both measurements must be the same. Thus, it is necessary to convert the mas of

aluminium used into litre. The conversion is based on the overall aluminium self-corrosion equation as shown in Eq.4.10.



Considering 1.3 V from Table 4.1, ideally, 1 g of aluminium was able to produce 1.245 L of hydrogen. In our study, a 0.0126 g of aluminium was used to produce 15.7ml of hydrogen gas. Aluminium efficiency can be calculated using Eq. 4.9, the solution is shown in Eq. 4.11. The rest of the information are calculated similarly and were used to plot Figure 4.11 and Figure 4.12.

$$1g \text{ Al} \left(\frac{1 \text{ mol Al}}{26.982} \right) \left(\frac{\frac{3}{2} \text{ mol H}_2}{1 \text{ mol Al}} \right) \left(\frac{22.4L}{1 \text{ mol H}_2} \right) = 1.245 L \quad (4.11)$$

$$\left(0.0126g \times \frac{1.245L}{1g} \right) = 0.0157L = 15.7 mL$$

$$\begin{aligned} \varepsilon &= 1 - \frac{8 mL}{15.7 mL} \\ &= 0.50 \times 100 \% \\ &= 50 \% \end{aligned}$$

From Figure 4.11, at high operating voltage, the hydrogen generation rate decreases rapidly until it reaches the equilibrium potential of water reduction, which is 1 V. Henceforth, the r_H is declining insignificantly. Taking into account both Figure 4.11 and Figure 4.12, higher electrolyte concentration contribute to higher hydrogen generation rate. Conversely, a high concentration electrolyte will cause a drop in efficiency level. Efficiency (ε) with KOH concentration of 1M and 2M starts to stabilize at 0.8 V and able to reach an astounding efficiency of more than 85 %. In 4M and 5M electrolyte case, the ε achieved is much lower about 80 % and 75 % respectively due to more OH^- . Theoretically, no hydrogen gas should be produced when voltage is lesser than 1.0 V.

The results recorded experience slight deviation because the hydrogen produced might have escaped to the surrounding affecting the data collection results. Another possibility is because the aluminium foil was folded into few layers, reaction might initial slower at some part of aluminium as electrolyte seep between the gaps.

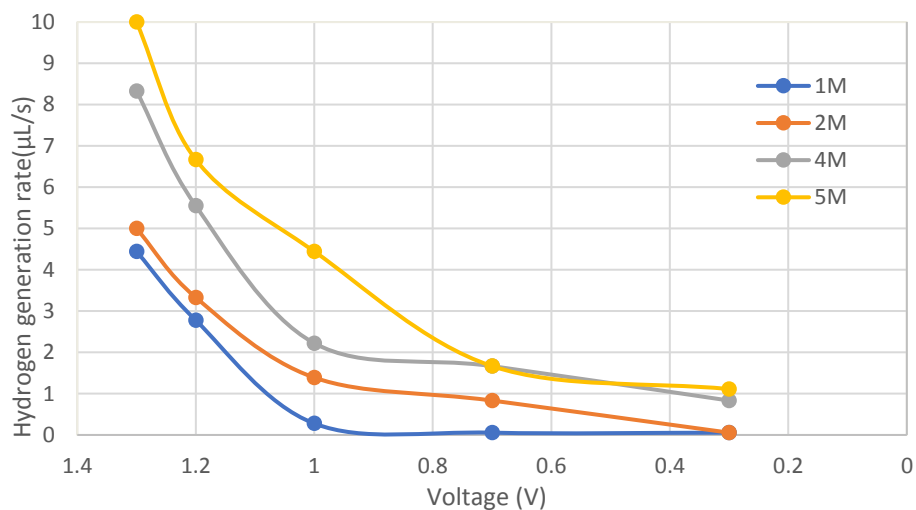


Figure 4.11: Hydrogen Generation Rate vs Voltage in Different Concentration of KOH.

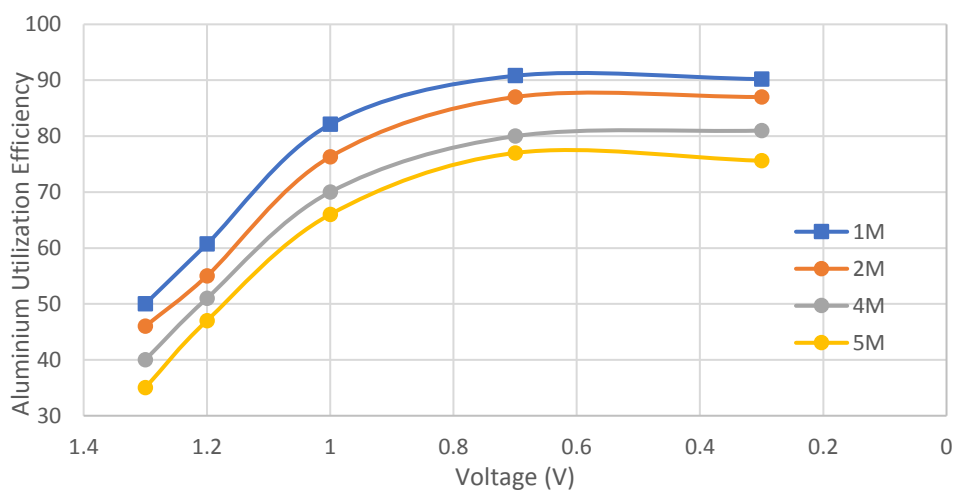


Figure 4.12: Aluminium Utilization Efficiency vs Voltage in Different Concentration of KOH.

From Figure 4.11, r_H is dependent on the concentration of electrolyte. A higher concentration of electrolyte contains more OH^- . From Eq. (4.1), a higher OH^- favours the forward direction to generate more hydrogen gas. This can be seen in Figure 4.11, under the same voltage, the hydrogen generation rate is higher when the concentration increases. Besides, from Eq. (4.3), aluminium oxidation rate increases when OH^- increases, leading to a higher short circuit current shown in polarization curve from Section 4.6. Unfortunately, the increase proportion from aluminium efficiency decreases as the concentration of electrolyte goes up due to more parasitic water reduction; which justify the reason behind the decrease in aluminium utilization efficiency as the concentration goes up in Figure 4.12. Thus, it can be deduced that the lesser volume of hydrogen gas collected leads to higher aluminium utilization efficiency.

The interaction between aluminium oxidation and water reduction can be discussed by applying mixed potential theory in electrochemical corrosion in this section, as shown in Figure 4.13 (Singh et al., 2010). From Eq. 4.1 and Eq.4.2, aluminium undergoes two redox couple namely the aluminium oxidation $\text{Al}/\text{Al}(\text{OH})_4^-$ and the parasitic water reduction $\text{H}_2/\text{H}_2\text{O}$. Voltage of aluminium, V_{Al} , represents by the green line while potential of parasitic, $E_{\text{corrosion}}$, represent by the red line. Theoretically, when reaction occurs, V_{Al} should have increases positively from -2.5 V. However, this was hinder by another couple reaction that undergoes parasitic reaction simultaneously, thus, a drastic drop in voltage can be seen. This justified the reason behind the huge difference of OCV in our study with theoretical model. The intersection of the aluminium oxidation and parasitic reaction indicates the open circuit condition of an aluminium air battery which is approximately -1.5 V vs Ag/AgCl as reference electrode (Liu et al., 2013).

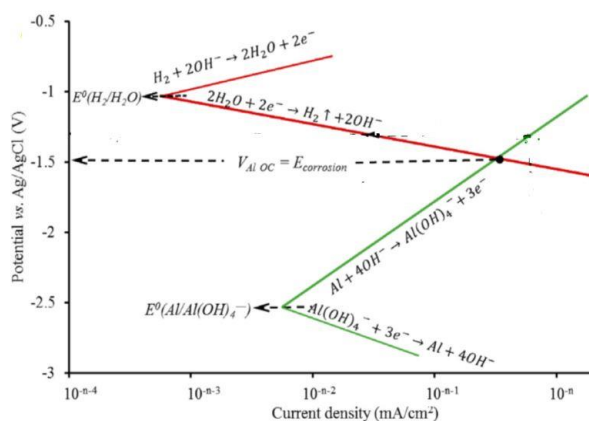


Figure 4.13: Theoretical model of aluminium reaction in alkaline solution.

When V_{Al} reaches -1 V, water reduction reaction reaches equilibrium state. Ideally, no hydrogen gas should be generated when V_{Al} is more positive than $E_{corrosion}$. Contrary to expectation, in this study, the aluminium anode was still releasing hydrogen gas when voltage drop below 1 V. This probably due to the fact that the kitchen type aluminium foil used contains impurity as depicted in Figure 4.14 and Figure 4.15. It is within expectation that aluminium foil contains many grain boundaries, dislocation and impurities on aluminium surface. Hence, this defective nature may be much more vulnerable to parasitic self-corrosion.

It is worth noting that some of the hydrogen gas is lost to the surrounding due to design fault when collecting the hydrogen, which justify the loss of efficiency. From Table 4.1, the slight decrease of efficiency at 0.3 V was because the volume of hydrogen gas was approximated to 1ml, which was in fact lesser than it; the minimum reading scale on the hydrogen collector is 1ml.

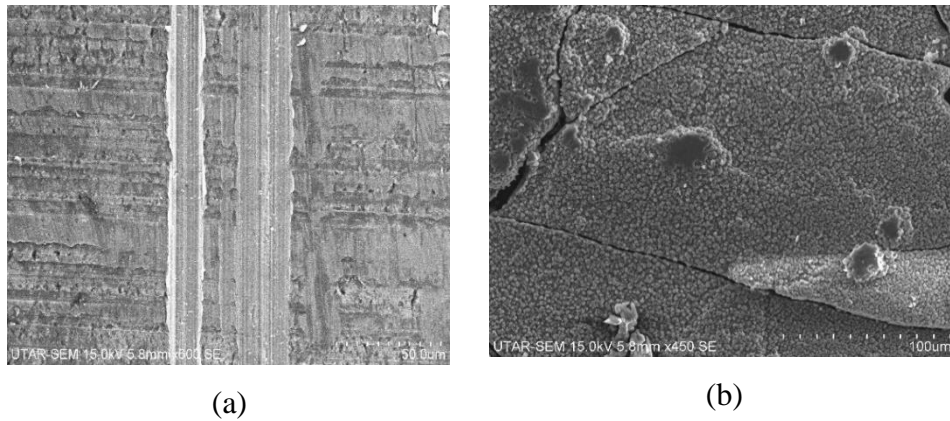
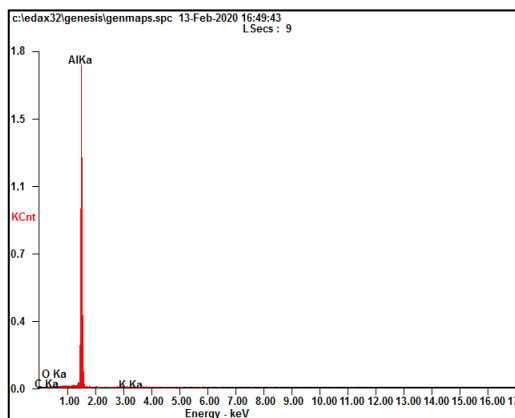
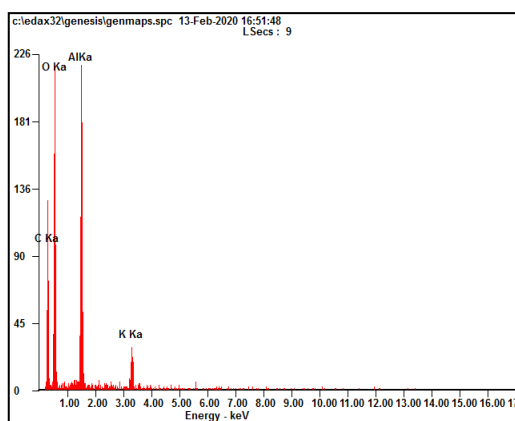


Figure 4.14: Images of Aluminium foil using SEM. (a) Aluminium kitchen foil before reaction (b) Aluminium foil after 24 hours of experiment.



(a)

| <i>Element</i> | <i>Wt%</i> | <i>At%</i> |
|----------------|------------|------------|
| <i>CK</i> | 00.36 | 00.80 |
| <i>OK</i> | 00.35 | 00.58 |
| <i>AlK</i> | 98.96 | 98.39 |
| <i>KK</i> | 00.33 | 00.23 |
| <i>Matrix</i> | Correction | MThin |



(b)

| <i>Element</i> | <i>Wt%</i> | <i>At%</i> |
|----------------|------------|------------|
| <i>CK</i> | 13.49 | 21.38 |
| <i>OK</i> | 41.37 | 49.22 |
| <i>AlK</i> | 33.97 | 23.96 |
| <i>KK</i> | 11.17 | 05.44 |
| <i>Matrix</i> | Correction | MThin |

Figure 4.15: EDX analysis and atomic weight composition on Aluminium (a) Before reaction (b) After 24hours of experiment.

4.6 Performance on Optimize System

4.6.1 Performance of Aluminium-air Sub-cell

The graph of voltage against current and power of the sub-cell is displayed in Figure 4.16. The OCV of the sub-cell was generally recorded only at 1.4 V. The short circuit current ranges from 40 mA to 86 mA as the electrolyte concentration increases from 1M to 5M. Generally, the polarization curves show an inverse proportional behaviour between cell voltage and current output. The voltage drop displayed by the cell is dominated by ohmic loss. The peak power density ranges from 13.8 mW to 37.8 mW with increasing electrolyte concentration due to more OH⁻ in higher concentration. The peak power occurs at 0.6 V in all electrolyte concentration.

In an operating alkaline aluminium-air battery, electron flow through the external circuit. Concurrently, bubbles of hydrogen gas continuously evolve on the surface of aluminium, some might be detained on the surface, which increase the resistance between aluminium electrode and the electrolyte (Liu et al., 2013). Besides, part of the overpotential is attributed to the resistance from the electrolyte. Based on research, obtained from APPENDIX B, the ionic conductivity of 1M KOH solution was measured to be 0.2153 S cm⁻¹ (Gilliam et al., 2007). Given that the gap between anode and cathode is 1cm, the solution resistance is calculated to be 4.6 Ω (=1 cm / 0.215 S cm⁻¹). Taking account for the maximum current output, the solution resistance contributes a maximum overpotential of 0.18 V (=4.6 Ω x 40 mA). Based on similar calculation, the solution resistance is expected to caused approximately 0.2 V maximum ohmic overpotential in each concentration of electrolyte.

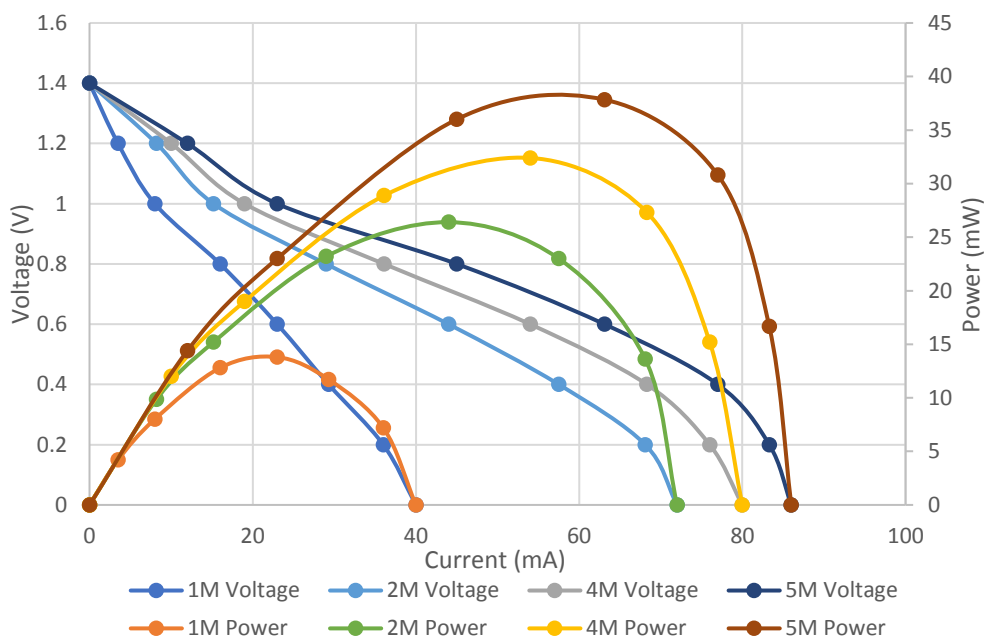


Figure 4.16: Polarization Curve of Aluminium/air Sub cell with Different Electrolyte Concentration.

4.6.2 Performance of Hydrogen/air Sub-cell

Figure 4.17 shows the performance of hydrogen/air Sub-cell plotted on a voltage and power against current graph. The sub-cell has a relatively small activation overpotential with OCV of 1.0V and short circuit current of 23.0 mA - 35.0 mA. The peak power ranges from 5.78 mW - 12.3 mW at a cell voltage of 0.55 V. A higher concentration of electrolyte will produce a higher current output. This can be justified by the improved kinetics reaction and increase in electrolyte conductivity due to the increase of OH^- . The mass transfer limitation occurs at 0.2 V due to reactant cannot be deliver to the active site fast enough. The distorted curve was due to the inconsistent transfer of hydrogen gas to the hydrogen anode.

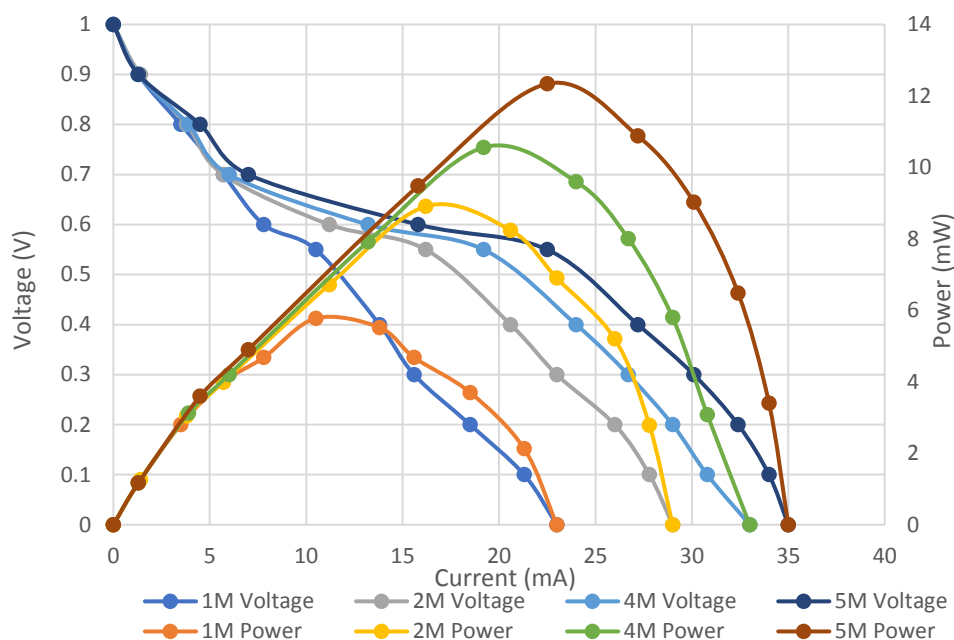


Figure 4.17: The Polarization curve of Hydrogen/air Sub-cell with Different Electrolyte Concentration

4.6.3 Overall System Efficiency Performance

The polarization results obtained can be explained from the model from Yang and Knickle from Figure 2.6 (Yang and Knickle, 2002). Aluminium-air battery main path involves the movement of electron from aluminium anode to cathode via external circuit, some electron was loss to hydrogen evolution parasitic reaction. This system assimilates an alternative path for the moving ions which involves hydrogen anode and gas diffusion cathode, producing electron. Overall, the electron flow from high energy level $\text{Al}/\text{Al}(\text{OH})^-$ to lower energy level O_2/OH^- . Instead of dissipating H_2 as exhaust it reutilizes it for electricity generation through the hydrogen/air sub-cell.

In this study, the hydrogen anode and aluminium air sub cell are interrelated by the hydrogen evolution reaction although both of them exhibit independent performance. Each-sub-cell can-have-its-own-power-output, thus, it's-possible-that-both sub-cells can operate under their-own-maximum-power simultaneously. The peak power of the hybrid-system can be obtained by adding both sub-cells as shown in Figure 4.19. From Table 4.2, the percentage increase for maximum power output is in the range of 32.5 % – 42 %, which indicate quite a significant advancement in performance. The maximum power

decreases-due to the increase-in-parasitic reaction and internal resistance (heat dissipated by the aluminium reaction).

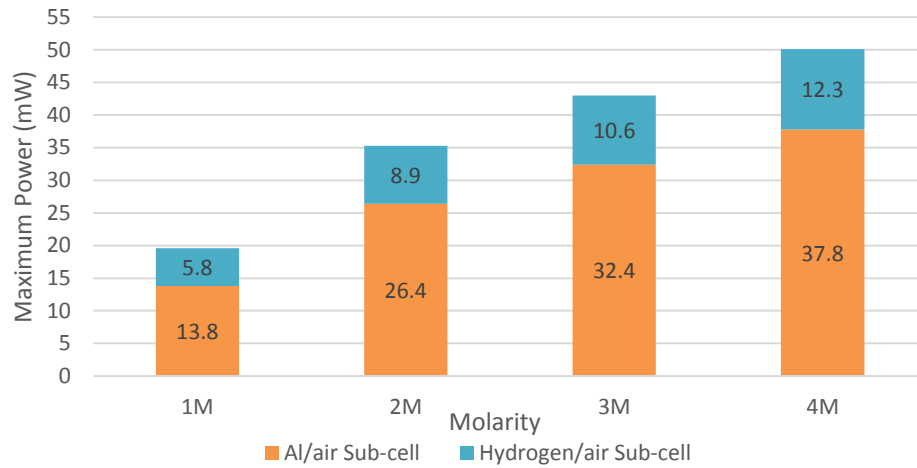


Figure 4.18: The Maximum Power Achieved at Different Concentration of Electrolyte.

Table 4.2: Peak Power Densities of Hybrid System.

| Electrolyte Concentration | Hybrid system P_{max} (mW) | Percentage increase of P_{max} (%) |
|---------------------------|------------------------------|--------------------------------------|
| 1 | 19.6 | 42.0 |
| 2 | 35.3 | 33.7 |
| 4 | 43.0 | 32.7 |
| 5 | 50.1 | 32.5 |

The efficiency of the whole system can be found by calculating the real efficiency of the fuel cell as shown in Eq. 4.12 (O'Hayre, 2016).

$$\begin{aligned} \varepsilon_{real} &= \varepsilon_{thermal} \times \varepsilon_{voltage} \times \varepsilon_{fuel} = \frac{\Delta\hat{g}}{\Delta\hat{h}} \times \frac{V}{E^0} \times \varepsilon_{fuel} \quad (4.12) \\ &= \frac{-nFV\varepsilon_{fuel}}{\Delta\hat{h}} \end{aligned}$$

Where:

n = mole number of valence electron, 3

F = Faraday constant, 96400 C mol⁻¹

$\Delta\hat{h}$ = enthalpy, -848000 J mol⁻¹

Based on Eq. 4.13, the cell efficiency for aluminium air is as follow:

$$\varepsilon_{Al\ cell} = \frac{-nFV\varepsilon}{\Delta\hat{h}} = 0.341\varepsilon V_{Al\ cell} \quad (4.13)$$

In order to calculate the whole system efficiency, hydrogen air sub-cell is incorporated into the calculation in Eq. 4.14.

$$\begin{aligned} \varepsilon_{system} &= \frac{-nF\varepsilon V_{Al\ cell} - nF(1 - \varepsilon) \times V_H\ cell}{\Delta\hat{h}} \quad (4.14) \\ &= \frac{-nF[\varepsilon V_{Al\ cell} + (1 - \varepsilon) \times V_H\ cell]}{\Delta\hat{h}} \\ &= \frac{-3 \times 96400 \times [\varepsilon V_{Al\ cell} + (1 - \varepsilon) \times V_H\ cell]}{-84800} \\ &= 0.341[\varepsilon V_{Al\ cell} + (1 - \varepsilon) \times V_H] \end{aligned}$$

From Figure 4.17, the hydrogen/air sub cell recorded the power peaks when the voltage, V_H , is 0.55 V. $V_{Al\ cell}$ at P_{max} can be found from Figure 4.16. The ε at P_{max} can be found by corresponding the voltage of aluminium, $V_{Al\ cell}$, from Figure 4.12 and the value of maximum power of voltage from Figure 4.16. $\varepsilon_{Al\ cell} \cdot \varepsilon_{system}$ was then calculated by using Eq. 4.13 and Eq. 4.14 respectively, the results were tabulated in Table 4.3.

Table 4.3: Efficiency of Hybrid System at Peak Power Densities.

| Electrolyte Concentration (M) | $V_{Al\ cell}$ at P_{max} (V) | ε at P_{max} (%) | Aluminium/air sub-cell efficiency $\varepsilon_{Al\ cell}$ (%) | Hybrid efficiency ε_{system} (%) |
|-------------------------------|---------------------------------|--------------------------------|--|--|
| 1 | 0.6 | 90.8 | 18.6 | 20.3 |
| 2 | 0.6 | 88 | 18.0 | 20.3 |
| 4 | 0.6 | 82 | 16.8 | 20.2 |
| 5 | 0.6 | 77 | 15.8 | 20.0 |

From Table 4.3, by incorporating hydrogen/air sub-cell, the efficiency of the hybrid system was enhanced by 20%. The system displays a rather stable

efficiency when tested with different electrolyte concentration. Therefore, it is suitable for application that required high power density output as they can operate under high electrolyte concentration without jeopardizing the overall system efficiency.

The efficiency was only increase slightly probably due to the fact that carbon dioxide is present in ambient air affecting the hydrogen/air sub-cell (Tewari et al., 2006). During reaction, carbon dioxide will react with potassium hydroxide electrolyte to form potassium carbonates within gas diffusion electrode, clogging the pores of the electrode leading to large performance drop (Kordesch and Sandstede, 1972). As shown in Figure 4.15(b) in which carbon was detected from the sample collected. This was verified by researchers, in which, maximum power density of fuel cell was dropped by half when the experiment was run on ambient air (145 mW) as compare to pure oxygen (Ma et al., 2014).

Apart from that, the hybrid system can operate on myriad application due to its merits of getting similar efficiency on different concentration of electrolyte. On the contrary, when higher concentration of electrolyte was used, the efficiency for the single aluminium/air sub-cell of the system degrades progressively. Therefore, the hybrid system is a cut above compare to the single sub-cell system at maximum power operation. Some of the application of high-power application are energy backup for power station and power generation for submarine.

4.6.4 Discharge Test Evaluation

The battery performance was also analysed from the discharge behaviour of Al-air battery at different discharge current at Figure 4.20. For constant discharge test, the cell discharge can be defined as in Eq. 4.15 (Cho et al., 2015). The calculated values of the cell discharge efficiency are presented in Table 4.4. The weight loss of aluminium is integrated into the equation, n and F denotes the valence electron of aluminium and Faraday constant respectively.

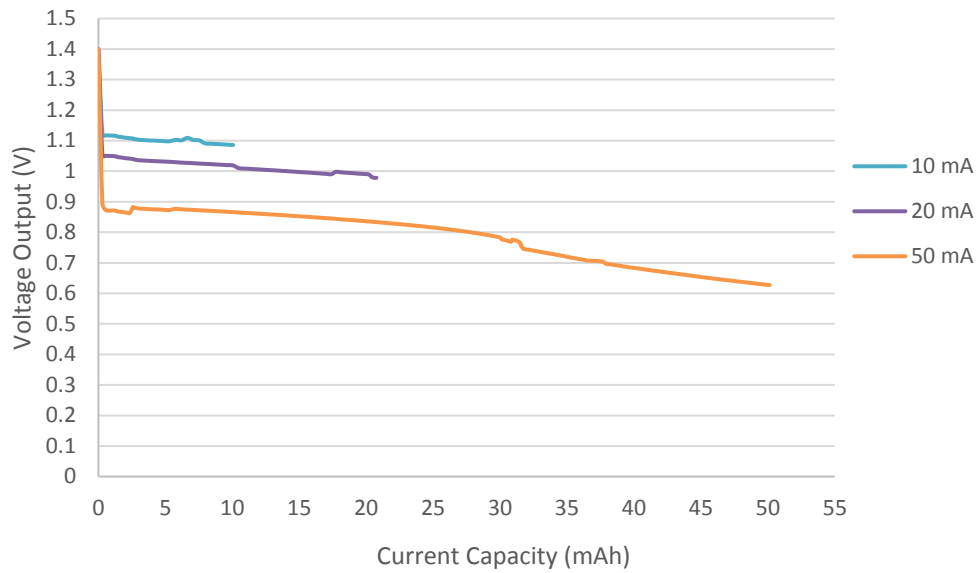


Figure 4.19: Graph of Voltage Output against Current Capacity at 10 mA, 20 mA and 50 mA Discharge Rate.

$$E_{wl} = \frac{n \times F \times \text{weight loss}}{\text{atomic weight}} \quad (4.15)$$

$$E_{real} = Q \times t$$

$$\eta_{al} = \frac{E_{real}}{E_{wl}} \times 100$$

Where

η_{al} = Efficiency

Q = Current capacity, A

t = Cutoff time, s

E_{real} = Electric capacity during discharge, C

E_{wl} = Electric capacity from weight loss, C

Table 4.4: The Discharge Efficiency of Cell at Different Discharge Current.

| Discharge Current | Electric capacity during discharge, E_{real} (C) | Electric capacity from weight loss, E_{wl} (C) | Efficiency, η_{al} (%) |
|-------------------|--|--|-----------------------------|
| 10 mA | 36.0 | 47.771 | 75.4 |
| 20 mA | 72.0 | 87.216 | 82.6 |
| 50 mA | 180.0 | 196.317 | 91.7 |

From Table 4.4, the efficiency of the cell recorded the highest at 50 mA while 10 mA was the lowest at 91.7 % and 75.4 % respectively. As indicated from the result, the efficiency increases with increasing discharge current. Most of the current was discharged through the main reaction, this is due to the fact that hydrogen evolution corrosion was insignificant and negligible at higher current density. Battery capacity is the amount of energy a battery can store. The discharge current is a non-linear power relationship with delivered capacity. This is the well know Peukert's effect which states that the greater the discharge rate, the lower the delivered capacity (Fan and Lu, 2015). As shown in Figure 4.20, a higher current shows a larger drop in voltage, decreasing the capacity of the cell. The internal resistance decreases with current and the voltage drop measured on the battery would increase with the current. This is due to the fact that at high current density, reactants cannot be delivered to the cathode quickly enough, thus, a more significant voltage drop can be seen as discharge current increase.

CHAPTER 5

CONCLUSIONS AND RECOMMENDATIONS

5.1 Conclusions

The aim and objectives of this project are achieved. A fusion of aluminium air battery and fuel cell hybrid prototype was designed and built; the performance of the hybrid cell was analysed. In Section 4.2, the hybrid cell prototype was constructed and a few tests were run such as performance test for each couple cell, standard electrode polarisation test and gas collection test; all the results have been analysed. In Section 4.4, the hybrid cell was optimised by changing the material and the dimension of the air cathode, consequently, the performance of the hybrid cell was improved significantly. In Section 4.5 and Section 4.6, aluminium utilization efficiency and overall performance cell test were conducted to measure and calculate the efficiency of the hybrid system. 1M, 2M, 4M and 5M of potassium hydroxide was used to study the effect of concentration of electrolyte on the performance of the hybrid cell. Aluminium air cell when connect in parallel or series, can produce sufficient power for small application such as flashlight, LED and glucometer (Avoundjian, Galvan and Gomez, 2017). A high-power hybrid cell, battery pack electrically connected by at least 2 single aluminium-air battery and electrolyte flow pump, is used as energy backup for power station (Wang et al., 2013).

In conclusion, a hybrid aluminium-air battery fuel cell was designed and built in this study to overcome the hydrogen-generating problem in alkaline aluminium air battery. From the preliminary test, the incorporation of hydrogen sub-cell has increased the peak power of the cell by 44 % from 6.2 mW to 8.93 mW. The result obtained was unsatisfactory. Thus, the system was modified by changing the air cathode to graphite felt. This has resulted in a great improvement for the peak power of the modified cell by 10.67 mW. The hybrid system achieved an increase of maximum power by 42 % from 13 mW to 19.6 mW. From cell polarization curve, the cell voltage decreases as current increases due to ohmic loss. The results obtained from polarization curve in efficiency test verifies that the aluminium utilization efficiency degrades with increasing

electrolyte concentration. When tested with different electrolyte, the percentage increase for maximum power output is in the range of 32.5 mW – 42 mW.

It is worth noting that the parasitic reaction has caused detrimental effects on the cell's open circuit voltage and also the whole system performance. Overall, with the embodiment of the fuel cell, the efficiency of the hybrid system was boosted up by 20%. The real efficiency of the system is stable, this may be accounted from the similar voltage recorded at different concentration of electrolyte when maximum power output is achieved. This provides clear evidence that it would not be of concern if high concentration electrolyte is needed for the applications. The discharge efficiency varies from 75.4 % - 91.7 % with increasing concentration of electrolyte. Most ions is being utilize, as they flow from aluminium anode to air cathode contributing producing electron via external circuit. This hybrid system has proven that low cost and a simple fabrication process is still capable to deliver a fully functional, light weight and long-lasting battery.

5.2 Recommendations for future work

The short life cycle of the hybrid system in this study was particularly due to limitation from the aluminium anode. In order to tackle this problem, aluminium will need to be stack in a few layers so that more reactant is available for oxidation, consequently, leading to longer discharge time (Liu et al., 2017b). This will lead to another recommendation, whereby the design of cell can further modify by increasing the size of the test rig to accommodate the stacked cell.

From the preliminary result, we can observe that the polarization curve for the aluminium was faltering due to the absent of platinum catalyst at the carbon cathode; because platinum is an expensive electrocatalyst. Catalyst such as platinum or palladium can be employed to better facilitate the oxygen reduction reaction.

From the optimised result, it is clearly shown that polarization of cell is dependent on the size of the electrode. One plausible assumption is that by increasing the size of air cathode, the surface area increases for intake of oxygen air and transfer of ions. Besides, having larger surface area can lower the internal resistance and increase the available maximum current of the cell. Besides, the

design for the whole prototype should be made bigger to accommodate the Ag/AgCl reference electrode in order to get a much more accurate results from the system instead of testing it at an external test rig.

Last but not least, carbon poisoning that blocking the pores on the surface of carbon cloth and graphite felt has deteriorate the performance of the hybrid cell. In future study, a system that supply oxygen should direct towards the air cathode to impede the formation of carbon on the surface, covering the pore of air cathode.

REFERENCES

- Abraham, K.M., 1993. Directions in secondary lithium battery research and development. *Electrochimica Acta*, 38(9), pp.1233–1248.
- Anon 2016. Chapter 2: Fuel Cell Thermodynamics. In: *Fuel Cell Fundamentals*. John Wiley & Sons, Ltd.pp.25–76.
- Avoundjian, A., Galvan, V. and Gomez, F.A., 2017. An inexpensive paper-based aluminum-air battery. *Micromachines*, 8(7).
- Brett, D.J.L., Aguiar, P., Brandon, N.P., Bull, R.N., Galloway, R.C., Hayes, G.W., Lillie, K., Mellors, C., Smith, C. and Tilley, A.R., 2006. Concept and system design for a ZEBRA battery-intermediate temperature solid oxide fuel cell hybrid vehicle. *Journal of Power Sources*, 157(2), pp.782–798.
- Briguglio, N., Andaloro, L., Ferraro, M. and Antonucci, V., 2011. Fuel Cell Hybrid Electric Vehicles. *Electric Vehicles – The Benefits and Barriers*, (May 2015).
- Buchel, K.H., Moretto, H.H. and Woditsch, P., 2000. *Industrial Inorganic Chemistry*. second ed. ed. Germany: Wiley-VCH.
- Cells, P.M.F., Potential, C., Output, P. and Barbir, F., 2013. Fuel Cell Efficiency Learn more about Fuel Cell Efficiency Fuel Cell Electrochemistry.
- Chawla, N., 2019. Recent advances in air-battery chemistries. *Materials Today Chemistry*, 12, pp.324–331.
- Chen, H., Cong, T.N., Yang, W., Tan, C., Li, Y. and Ding, Y., 2009. Progress in electrical energy storage system: A critical review. *Progress in Natural Science*, 19(3), pp.291–312.
- Cho, Y.J., Park, I.J., Lee, H.J. and Kim, J.G., 2015. Aluminum anode for aluminum-air battery - Part I: Influence of aluminum purity. *Journal of Power Sources*, 277, pp.370–378.
- Ding, F., Zong, J., Wang, S., Zhong, H., Zhang, Q. and Zhao, Q., 2016. *Aluminum–Air Batteries*.
- Durmus, Y.E., Montiel Guerrero, S.S., Aslanbas, Ö., Tempel, H., Hausen, F., de Haart, L.G.J., Ein-Eli, Y., Eichel, R.A. and Kungl, H., 2018. Investigation of the corrosion behavior of highly As-doped crystalline Si in alkaline Si-air batteries. *Electrochimica Acta*, 265, pp.292–302.

Egan, D.R., Ponce De León, C., Wood, R.J.K., Jones, R.L., Stokes, K.R. and Walsh, F.C., 2013. Developments in electrode materials and electrolytes for aluminium-air batteries. *Journal of Power Sources*, 236, pp.293–310.

Fan, L. and Lu, H., 2015. The effect of grain size on aluminum anodes for Al-air batteries in alkaline electrolytes. *Journal of Power Sources*, 284, pp.409–415.

Gauchia, L., Bouscayrol, A., Sanz, J., Trigui, R. and Barrade, P., 2011. Fuel cell, battery and supercapacitor hybrid system for electric vehicle: Modeling and control via energetic macroscopic representation. *2011 IEEE Vehicle Power and Propulsion Conference, VPPC 2011*, pp.1–6.

Gilliam, R.J., Graydon, J.W., Kirk, D.W. and Thorpe, S.J., 2007. A review of specific conductivities of potassium hydroxide solutions for various concentrations and temperatures. *International Journal of Hydrogen Energy*, 32(3), pp.359–364.

Goodenough, J.B., 2014. Electrochemical energy storage in a sustainable modern society. *Energy and Environmental Science*, 7(1), pp.14–18.

Jeong, K.S. and Oh, B.S., 2002. Fuel economy and life-cycle cost analysis of a fuel cell hybrid vehicle. *Journal of Power Sources*, 105(1), pp.58–65.

Jiang, H.R., Shyy, W., Wu, M.C., Zhang, R.H. and Zhao, T.S., 2019. A biporous graphite felt electrode with enhanced surface area and catalytic activity for vanadium redox flow batteries. *Applied Energy*, 233–234(September 2018), pp.105–113.

Kane, S.N., Mishra, A. and Dutta, A.K., 2016. Preface: International Conference on Recent Trends in Physics (ICRTP 2016). *Journal of Physics: Conference Series*, 755(1).

Khaligh, A. and Li, Z., 2010. Battery, ultracapacitor, fuel cell, and hybrid energy storage systems for electric, hybrid electric, fuel cell, and plug-in hybrid electric vehicles: State of the art. *IEEE Transactions on Vehicular Technology*, 59(6), pp.2806–2814.

Khan, Z., Parveen, N., Ansari, S.A., Senthilkumar, S.T., Park, S., Kim, Y., Cho, M.H. and Ko, H., 2017. Three-dimensional SnS₂ nanopetals for hybrid sodium-air batteries. *Electrochimica Acta*, 257, pp.328–334.

Kordesch, K.V. and Sandstede, G., 1972. *Electrocatalysis to Fuel Cells*.

Lakshminathiraj, P., G.Bhaskar, R., Basariya, M.R., Parvathy, S. and Swarna, P., 2008. Removal of Cr (VI) by electrochemical reduction. *Separation and*

Purification Technology, 60, pp.96–102.

Lee, J., Kim, S.T., Cao, R., Choi, N., Liu, M. and Lee, K.T., 2011. Metal – Air Batteries with High Energy Density : Li – Air versus Zn – Air. pp.34–50.

Li, Q., Mahmood, N., Zhu, J., Hou, Y. and Sun, S., 2014. Graphene and its composites with nanoparticles for electrochemical energy applications. *Nano Today*, 9(5), pp.668–683.

Libich, J., Máca, J., Vondrák, J., Čech, O. and Sedlaříková, M., 2018. Supercapacitors: Properties and applications. *Journal of Energy Storage*, 17(March), pp.224–227.

Liu, F., Wang, W., Wang, L. and Yang, G., 2013. Working principles of solar and other energy conversion cells. *Nanomaterials and Energy*, 2(1), pp.3–10.

Liu, Y., Sun, Q., Li, W., Adair, K.R., Li, J. and Sun, X., 2017a. A comprehensive review on recent progress in aluminum–air batteries. *Green Energy and Environment*, 2(3), pp.246–277.

Liu, Z., Zhao, J., Cai, Y. and Xu, B., 2017b. Design and research on discharge performance for aluminum-air battery. *AIP Conference Proceedings*, 1794(January).

Lucia, U., 2014. Overview on fuel cells. *Renewable and Sustainable Energy Reviews*, 30, pp.164–169.

Ma, X., Yang, H., Yu, L., Chen, Y. and Li, Y., 2014. Preparation, surface and pore structure of high surface area activated carbon fibers from bamboo by steam activation. *Materials*, 7(6), pp.4431–4441.

Marcilio, N.R., Tessaro, I.C. and Gerchmann, M., 2012. Production of hydrogen in the reaction between aluminum and water in the presence of NaOH and KOH. *Brazilian Journal of Chemical Engineering*, 29, pp.337–348.

Nestoridi, M., Pletcher, D., Wood, R.J.K., Wang, S., Jones, R.L., Stokes, K.R. and Wilcock, I., 2008. The study of aluminium anodes for high power density Al/air batteries with brine electrolytes. *Journal of Power Sources*, 178(1), pp.445–455.

Offer, G.J., Howey, D., Contestabile, M., Clague, R. and Brandon, N.P., 2010. Comparative analysis of battery electric, hydrogen fuel cell and hybrid vehicles in a future sustainable road transport system. *Energy Policy*, 38(1), pp.24–29.

Padbury, R. and Zhang, X., 2011. Lithium-oxygen batteries - Limiting factors that affect performance. *Journal of Power Sources*, 196(10), pp.4436–4444.

Pan, W., Wang, Y., Kwok, H.Y.H. and Leung, D.Y.C., 2019. A low-cost portable cotton-based aluminum-air battery with high specific energy. *Energy Procedia*, 158, pp.179–185.

Park, I.J., Choi, S.R. and Kim, J.G., 2017. Aluminum anode for aluminum-air battery – Part II: Influence of In addition on the electrochemical characteristics of Al-Zn alloy in alkaline solution. *Journal of Power Sources*, 357, pp.47–55.

Patnaik, R.S.M., Ganesh, S., Ashok, G., Ganesan, M. and Kapali, V., 1994. Heat management in aluminium/air batteries: sources of heat. *Journal of Power Sources*, 50(3), pp.331–342.

Pei, P., Wang, K. and Ma, Z., 2014. Technologies for extending zinc-air battery's cyclelife: A review. *Applied Energy*, 128, pp.315–324.

Peng, B. and Chen, J., 2009. Functional materials with high-efficiency energy storage and conversion for batteries and fuel cells. *Coordination Chemistry Reviews*, 253(23–24), pp.2805–2813.

Pollet, B.G., Staffell, I. and Shang, J.L., 2012. Current status of hybrid, battery and fuel cell electric vehicles: From electrochemistry to market prospects. *Electrochimica Acta*, 84, pp.235–249.

Revel, R., Audichon, T. and Gonzalez, S., 2014. Non-aqueous aluminium e air battery based on ionic liquid electrolyte. *Journal of Power Sources*, 272, pp.415–421.

Schmidt-Rohr, K., 2018. How Batteries Store and Release Energy: Explaining Basic Electrochemistry. *Journal of Chemical Education*, 95(10), pp.1801–1810.

Sharaf, O.Z. and Orhan, M.F., 2014. An overview of fuel cell technology: Fundamentals and applications. *Renewable and Sustainable Energy Reviews*, 32, pp.810–853.

Singh, D., Pratap, D., Baranwal, Y., Kumar, B. and Chaudhary, R.K., 2010. Microbial fuel cells: A green technology for power generation. *Annals of Biological Research*, 1(3), pp.128–138.

Soler, L., Macanás, J., Muñoz, M. and Casado, J., 2007. Aluminum and aluminum alloys as sources of hydrogen for fuel cell applications. *Journal of Power Sources*, 169(1), pp.144–149.

Strauß, C., Vetter, A. and Von Felde, A., 2012. BiogasbiogasProductionbiogasproductionand Energy Cropsbiogasenergy crops. In: R.A. Meyers, ed. *Encyclopedia of Sustainability Science and Technology*. New York, NY: Springer New York.pp.1097–1145.

Sun, Q., Yang, Y. and Fu, Z.W., 2012. Electrochemical properties of room temperature sodium-air batteries with non-aqueous electrolyte. *Electrochemistry Communications*, 16(1), pp.22–25.

Tewari, A., Sambhy, V., Urquidi MacDonald, M. and Sen, A., 2006. Quantification of carbon dioxide poisoning in air breathing alkaline fuel cells. *Journal of Power Sources*, 153(1), pp.1–10.

Wang, B., Shi, J., Shi, Y., Narayanan, S. and Koratkar, N., 2018. of lithium dendrites. 1516(March), pp.1513–1516.

Wang, L., Wang, W., Yang, G., Liu, D., Xuan, J., Wang, H., Leung, M.K.H. and Liu, F., 2013. A hybrid aluminum/hydrogen/air cell system. *International Journal of Hydrogen Energy*, 38(34), pp.14801–14809.

Wehrey, M.C., 2004. What's new with hybrid electric vehicles. *IEEE Power and Energy Magazine*, 2(6), pp.34–39.

Winter, M. and Brodd, R.J., 2004a. What are batteries, fuel cells, and supercapacitors? *Chemical Reviews*, 104(10), pp.4245–4269.

Winter, M. and Brodd, R.J., 2004b. What are batteries, fuel cells, and supercapacitors? *Chemical Reviews*, 104(10), pp.4245–4269.

Yang, S., 2003. Design and analysis of aluminum/air battery system for electric vehicles. *Journal of Power Sources*, 112(1), pp.162–173.

Yang, S. and Knickle, H., 2002. Design and analysis of aluminum/air battery system for electric vehicles. *Journal of Power Sources - J POWER SOURCES*, 112, pp.162–173.

Yin, W.W. and Fu, Z.W., 2017. The Potential of Na–Air Batteries. *ChemCatChem*, 9(9), pp.1545–1553.

YU, K., YANG, S., XIONG, H., WEN, L., DAI, Y., TENG, F. and FAN, S., 2015. Effects of gallium on electrochemical discharge behavior of Al–Mg–Sn–In alloy anode for air cell or water-activated cell. *Transactions of Nonferrous Metals Society of China*, 25(11), pp.3747–3752.

Zaromb, S., 1963. The Use and Behavior of Aluminum Anodes in Alkaline Primary Batteries.

Zhang, J., Klasky, M. and Letellier, B., 2009. The aluminum chemistry and corrosion in alkaline solutions. *Journal of Nuclear Materials*, 384, pp.175–189.

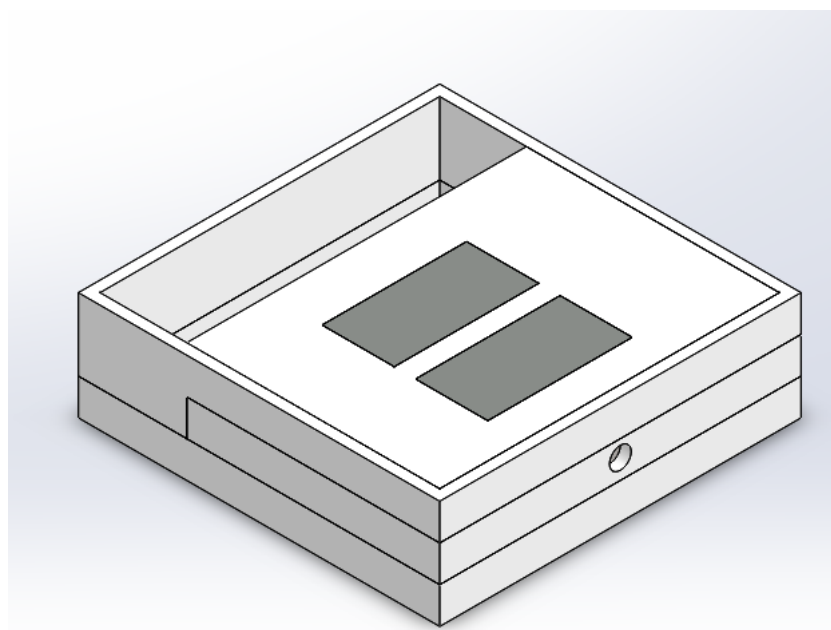
Zhang, X., Wang, X.G., Xie, Z. and Zhou, Z., 2016a. Recent progress in

rechargeable alkali metal–air batteries. *Green Energy and Environment*, 1(1), pp.4–17.

Zhang, X., Wang, X.G., Xie, Z. and Zhou, Z., 2016b. Recent progress in rechargeable alkali metal–air batteries. *Green Energy and Environment*, 1(1), pp.4–17.

Zhao, Z., Yuan, Z., Fang, Z., Jian, J., Li, J., Yang, M., Mo, C., Zhang, Y., Hu, X., Li, P., Wang, S., Hong, W., Zheng, Z., Ouyang, G., Chen, X. and Yu, D., 2018. In Situ Activating Strategy to Significantly Boost Oxygen Electrocatalysis of Commercial Carbon Cloth for Flexible and Rechargeable Zn-Air Batteries. *Advanced Science*, 5(12).

APPENDICES



APPENDIX A: The conceptual design of hybrid system

 Calculated values of specific conductivity in (S/cm) at various concentrations (M) and temperatures (°C)

| Concentration (M) | Temperature (°C) | | | | | | | |
|-------------------|------------------|---------|---------|---------|---------|---------|---------|---------|
| | 0 | 10 | 20 | 25 | 30 | 40 | 50 | 60 |
| 0.01 | 0.00174 | 0.00200 | 0.00229 | 0.00243 | 0.00259 | 0.00290 | 0.00323 | 0.00357 |
| 0.02 | 0.00347 | 0.00400 | 0.00457 | 0.00486 | 0.00517 | 0.00579 | 0.00645 | 0.00713 |
| 0.03 | 0.00520 | 0.00599 | 0.00684 | 0.00728 | 0.00774 | 0.00868 | 0.00967 | 0.0107 |
| 0.05 | 0.00864 | 0.0100 | 0.0114 | 0.0121 | 0.0129 | 0.0144 | 0.0161 | 0.0178 |
| 0.1 | 0.0171 | 0.0198 | 0.0226 | 0.0241 | 0.0256 | 0.0287 | 0.0320 | 0.0354 |
| 0.2 | 0.0338 | 0.0390 | 0.0446 | 0.0476 | 0.0506 | 0.0568 | 0.0633 | 0.0700 |
| 0.3 | 0.0500 | 0.0578 | 0.0661 | 0.0705 | 0.0750 | 0.0842 | 0.0939 | 0.1040 |
| 0.5 | 0.0808 | 0.0937 | 0.1074 | 0.1146 | 0.1220 | 0.1373 | 0.1532 | 0.1698 |
| 1 | 0.1499 | 0.1747 | 0.2013 | 0.2153 | 0.2296 | 0.2592 | 0.2901 | 0.3222 |
| 2 | 0.2556 | 0.3020 | 0.3518 | 0.3778 | 0.4046 | 0.4602 | 0.5183 | 0.5786 |
| 3 | 0.3235 | 0.3881 | 0.4576 | 0.4940 | 0.5315 | 0.6093 | 0.6907 | 0.7752 |
| 4 | 0.3598 | 0.4392 | 0.5250 | 0.5700 | 0.6164 | 0.7128 | 0.8136 | 0.9184 |
| 5 | 0.3708 | 0.4617 | 0.5603 | 0.6121 | 0.6656 | 0.7768 | 0.8933 | 1.0144 |
| 6 | 0.3627 | 0.4618 | 0.5697 | 0.6266 | 0.6853 | 0.8077 | 0.9360 | 1.0696 |
| 7 | 0.3417 | 0.4457 | 0.5594 | 0.6196 | 0.6818 | 0.8117 | 0.9481 | 1.0901 |
| 8 | 0.3142 | 0.4197 | 0.5359 | 0.5976 | 0.6614 | 0.7950 | 0.9356 | 1.0822 |
| 9 | 0.2864 | 0.3900 | 0.5052 | 0.5666 | 0.6304 | 0.7640 | 0.9050 | 1.0522 |
| 10 | 0.2646 | 0.3630 | 0.4737 | 0.5331 | 0.5949 | 0.7249 | 0.8625 | 1.0063 |
| 11 | 0.2550 | 0.3449 | 0.4476 | 0.5032 | 0.5612 | 0.6839 | 0.8142 | 0.9508 |
| 12 | 0.2638 | 0.3419 | 0.4332 | 0.4832 | 0.5357 | 0.6473 | 0.7666 | 0.8920 |

APPENDIX B: Specific conductivity of KOH at different temperature and concentration.